

# Relay Control for Full-Duplex Relaying with Wireless Information and Energy Transfer

Hongwu Liu, *Member, IEEE* Kyeong Jin Kim, *Senior Member, IEEE*,  
and Kyung Sup Kwak, *Member, IEEE*

## Abstract

This paper investigates the wireless information and energy transfer for the dual-hop amplify-and-forward full-duplex relaying system. By considering the time switching relay transceiver architecture, the full duplex information relaying is powered via the energy harvested from the source-emitted radio frequency signal. The throughput performances of three relay control schemes, namely, the maximum relay gain, the optimal relay gain, and the target relay gain are investigated. The analytical expressions for the outage probability and the ergodic capacity are presented for all the three relay control schemes. The time switching factors for the optimal relay gain and the target relay gain are, respectively, presented in closed-form. The analytical and numerical results show that the optimal relay gain and the target relay gain achieve better outage performances than the maximum relay gain. The optimal relay gain achieves a higher ergodic capacity than that of the maximum relay gain in high signal-to-noise ratios, while the target relay gain achieves a competitive ergodic capacity without requiring the second-hop channel condition. Compared with the maximum relay gain employing the numerically optimized time switching, the competitive throughput performances are achieved by the optimal relay gain and the target relay gain, respectively. It also observes that when the relay is placed in the middle of the source and the destination, the maximum relay gain and the optimal relay gain achieve the relatively worse throughput performance, while the throughput decreases dramatically for the target relay gain when the relay moves from the source towards the destination.

## Index Terms

Energy harvesting, wireless power transfer, amplify-and-forward, full-duplex relay, gain control.

Hongwu Liu is with Shandong Jiaotong University, Jinan, China (e-mail: hong.w.liu@hotmail.com).

K. J. Kim is with Mitsubishi Electric Research Laboratories (MERL), 201 Broadway, Cambridge, MA 02139 (e-mail: kyeong.j.kim@hotmail.com).

K. S. Kwak are with Inha University, Incheon, Korea (e-mail: kskwak@inha.ac.kr).

## I. INTRODUCTION

Recently, energy harvesting (EH) has emerged as a promising approach to prolong the lifetime of energy constrained wireless communications [1]–[3]. Through harvesting energy from the natural sources (e.g., solar, wind, thermoelectric effects or other physical phenomena), periodical battery replacement or recharging could be alleviated in conventional EH-aided wireless communications [1]–[4]. However, EH from natural sources is vulnerable to environmental changes such that conventional EH-aided wireless communications are currently far from convenient, stable, and reliable [4]. With the capability of harvesting energy from ambient radio-frequency (RF) signals, simultaneous wireless information and energy transfer (SWIET) provides a more encouraging way than conventional EH-aided wireless communications to work in the physical or economic limited environments [5]–[11].

The pioneering works on SWIET can be traced back to [5] and [6], where the fundamental tradeoff between the capacity and energy was studied for the point-to-point communication scenarios. Following the assumption that an ideal receiver is capable of observing information and extracting energy from the same received signals, SWIET has been extended for multi-antenna systems [12], multiuser systems [13], and bi-directional communication systems [14], respectively. However, as discussed in [7], a practical circuit for EH from an RF signal could hardly decode the carried information from the same signal. Therefore, [7] proposed two practical receiver architectures, namely, time switching (TS) and power splitting (PS), which are now widely adopted in various wireless systems, such as multiple-input multiple-out (MIMO) systems [15], orthogonal frequency division multiplexing (OFDM) systems [16], and cellular systems [8].

In parallel with the above researches mainly dealing with the single-hop scenarios, employing intermittent relays to facilitate RF EH and information transfer in wireless cooperative or sensor networks has also draw significant attention [9]–[11], [17]–[19]. The importance of relay-based SWIET lies in the fact that, not only does it enable wireless communications over long distances or across barriers, but it keeps the energy-constrained relays active through RF EH. The authors of [11] designed and analyzed TS and PS relay protocols for amplify-and-forward (AF) relaying systems, and later on, the same authors extended TS relay protocol to an adaptive one [20]. Also, TS and PS relay protocols have been extended for non-regenerative MIMO-OFDM relay systems [19]. In [10], the throughput performances of TS and PS relay protocols for decode-and-

forward (DF) relaying were investigated. In [21], power allocation strategies for EH relay systems with multiple source-destination pairs were studied. The outage and diversity performances of SWIET for cooperative networks with spatially random relays were investigated in [22] and the distributed PS-based SWIET was designed for interference relay systems [23]. More recently, antenna switching and antenna selection for SWIET relaying systems have been investigated in [24] and [25], respectively. Nevertheless, all these works are limited to the half-duplex relaying (HDR) mode. Since the source-to-relay and the relay-to-destination channels are kept orthogonal by either frequency division or time division multiplexing, significant loss of spectrum efficiency takes place in HDR mode. As an alternative, full-duplex relaying (FDR) has draw much attention [26]–[30]. Since FDR requires only one channel use for the end-to-end transmission, great improvement of spectrum efficiency can be achieved.

So far, quite a few works have been done for SWIET in the FDR systems. In [28], throughput performance of TS relaying protocol has been analyzed for the FDR SWIET systems, where the scenarios of relay EH with single and dual antennas were considered, respectively. In practice, since the relay node suffers severe self-interference (loop interference) from its own transmit signal, FDR operation is difficult to implement. For example, more than 106 dB self-interference has to be suppressed by a femto-cell FDR base-station to achieve the link signal-to-noise-ratio (SNR) equal to that of a HDR counterpart [31]. For the systems requiring a higher transmit power, more self-interference suppression is needed [26]. By employing relay EH in the second time phase for the conventional two-phase AF HDR systems, [32] proposed a self-interference immunized full-duplex relay node, which can transmit information and extract energy simultaneously with different antennas. Another important issue for SWIET is to determinate the EH parameters, i.e., the TS factor and the PS factor for TS and PS relay protocols, respectively. For TS relay protocol, the determination of the TS factor affects not only the relay-harvested energy, but also the effective relaying transmission time. Compared with PS relay protocol, TS relay protocol is more practical due to its simplicity. With the aid of statistic channel state information (CSI), the numerical optimizations of the TS factor has been presented in [11], [28]. In the delay-limited and delay-tolerant transmission modes, the instantaneous CSI can also be applied to optimize the EH parameter, as well as the instantaneous CSI-aided transmission power control in the FDR systems [29], [30].

Motivated by this, we focus on wireless information and energy transfer for a dual-hop FDR

system, where the TS-based AF relay node is powered via EH from the source-emitted RF signal. Compared with previous works, some distinct features of our work are stressed here. In [32], the effective time of information transmission is the same as that of the HDR systems. Therefore, the spectrum efficiency improvement achieved by the scheme of [32] is small compared to that of the FDR systems. Following the scheme of the full usage of the relay transmission power, the authors of [28] designed wireless information and energy transfer for the FDR systems, where the relay node adopts the the maximum relay gain [27], [33]. Then, the achievement of the maximum throughput becomes a TS optimization problem, which in general doesn't have a closed-form solution [28]. In this paper, three relay control schemes, namely, the maximum relay gain, the optimal relay gain, and the target relay gain are investigated for the instantaneous transmission, the delay-limited transmission, and the delay-tolerant transmission modes, respectively. The contributions of this work are summarized as follows:

- The end-to-end signal-to-interference-plus-noise-ratio (SINR) is formulated as a non-linear function of the relay gain and the TS factor. The optimal relay gain and the target relay gain are designed to maximize the end-to-end SINR and to achieve the target end-to-end SINR, respectively. With the obtained closed-form TS factors for the optimal relay gain and the target relay gain, the instantaneous CSI can be utilized to improve the system throughput in the delay-limited transmission and the delay-tolerant transmission modes, respectively.
- We present analytical expressions of the system throughput for all the three relay control schemes in the instantaneous transmission, the delay-limited transmission, and the delay-tolerant transmission modes, respectively. Specifically, analytical expressions of the outage probability are derived for all the three relay control schemes in the delay-limited mode, while analytical expressions of the ergodic capacity are derived for all the three relay control schemes in the delay-tolerant mode.
- In high interference-to-noise-ratios (INRs), the optimal relay gain with the closed-form TS achieves the same instantaneous throughput as that of the maximum relay gain with the numerically optimized TS. In the delay-limited mode, the optimal relay gain and the target relay gain achieve the better outage performances than the maximum relay gain. In the delay-tolerant mode, the optimal relay gain achieves a higher ergodic capacity than the maximum relay gain in high SNRs, while the target relay gain achieves a competitive

ergodic capacity without requiring the second-hop channel condition. Compared with the maximum relay gain, the competitive throughput performances are achieved by the optimal relay gain and the target relay gain, respectively.

- We provide numerical results to show that the throughput performances for the maximum relay gain and the optimal relay gain are relatively worse when the relay is placed in the middle of the source and the destination, while for the target relay gain with a high target SINR, the throughput monotonically decreases when the relay moves from the source towards the destination. In the delay-tolerant mode, it is also shown that for any two relay nodes at the symmetric positions of the middle of the source and the destination, the relay near the source achieves a higher throughput than that of the relay near the destination.

The rest of the paper is organized as follows. Section II describes the system model of the FDR system and formulates the throughput optimization problem. Section III presents the three relay control schemes. The analytical results of the system throughput are presented in Section IV. Section V presents some numerical results and discuss the system performances of our proposed relay control schemes. Finally, Section VI summarizes this work.

## II. SYSTEM MODEL

A wireless dual-hop FDR system is considered, where a source node wants to transfer its information to the destination node. Due to the large distance or the barrier between the source and the destination, an intermediate relay is applied to assist the information transmission from the source to the destination. The intermediate relay is assumed to be an energy constrained device such that it has to harvest energy from the source-emitted RF signal to forward the source information to the destination. For the purpose of implementation simplicity, AF relaying scheme and TS transceiver architecture are chosen at the relay node. The channel coefficients from the source to the relay and from the relay to the destination are denoted by  $h$  and  $g$ , respectively. The loopback interference channel at the relay node is denoted by  $f$ . All the channels are assumed to be frequency non-selective and quasi-static block-fading, following a Rayleigh distribution. The means of the exponential random variables  $|f|^2$ ,  $|g|^2$ , and  $|h|^2$  are denoted by  $\lambda_f$ ,  $\lambda_g$ , and  $\lambda_h$ , respectively. By utilizing the pilots sent from the source over the dual-hop link, the dual-hop CSI can be estimated to facilitate the wireless information and energy transfer [7], [10], [11], [15], [32]. In order to explore the potential capacity and performance limit of such an AF FDR

system, we assume that a centralized entity having access to the ideal global (or partial) CSI will compute and update the relay control parameters.

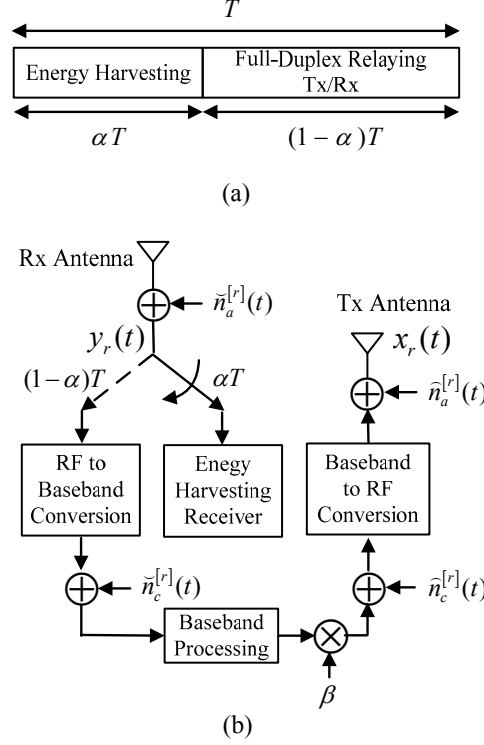


Fig. 1. (a) Illustration of the key parameters for EH and FDR at the relay. (b) Block diagram of the relay transceiver.

The framework of TS relay protocol is illustrated in Fig. 1(a), in which each time block  $T$  is divided into two phases. Denote the TS factor by  $\alpha$  ( $0 < \alpha < 1$ ), the first phase is assigned with a duration of  $\alpha T$ , which is used for energy transfer from the source to the relay. The second phase is assigned with a duration of  $(1 - \alpha)T$ , which is used for full-duplex information relaying via the dual-hop channel. The relay-received RF signal in the two time phases are sent to the EH receiver and the full-duplex transceiver, respectively, as illustrated in Fig. 1(b). Note that during the first time phase, the relay node does not transmit. Thus, no loop interference is introduced during the EH period to the relay-received RF signal. The harvested energy at the relay is given by [7]

$$E_h = \frac{\eta P_s |h|^2}{d_1^m} \alpha T, \quad (1)$$

where  $P_s$  is the source transmit power,  $d_1$  is the distance between the source and the relay,

$m$  is the path loss exponent, and  $\eta$  is the energy conversion efficiency which depends on the EH circuitry and the rectification process. When the relay node operates in the FDR mode, it concurrently receives the signal  $y_r(t)$  and transmits the signal  $x_r(t)$  on the same frequency. As depicted in Fig. 2(b), the full-duplex transceiver down-converts the received RF signal to baseband, processes the baseband signal, and up-converts the processed baseband signal. In Fig. 2(b),  $\tilde{n}_a^{[r]}(t)$  and  $\hat{n}_a^{[r]}(t)$  are the narrow-band Gaussian noises introduced by the receiving and transmitting antennas, respectively,  $\tilde{n}_c^{[r]}(t)$  and  $\hat{n}_c^{[r]}(t)$  are the baseband additive white Gaussian noises (AWGNs) due to down-conversion and up-conversion, respectively [7]. For simplicity, the equivalent baseband noise due to the effects of both  $\tilde{n}_a^{[r]}(t)$  and  $\hat{n}_a^{[r]}(t)$  is modeled by the zero mean AWGN  $n_a^{[r]}(t)$  with variance  $\sigma_{n_a^{[r]}}^2$ , and the equivalent baseband noise due to the effects of both  $\tilde{n}_c^{[r]}(t)$  and  $\hat{n}_c^{[r]}(t)$  is modeled by the zero mean AWGN  $n_c^{[r]}(t)$  with variance  $\sigma_{n_c^{[r]}}^2$ . Therefore, the overall AWGN at the relay node can be modeled as the zero mean AWGN  $n_r(k) \triangleq n_a^{[r]}(k) + n_c^{[r]}(k)$  with variance  $\sigma_r^2 \triangleq \sigma_{n_a^{[r]}}^2 + \sigma_{n_c^{[r]}}^2$ . At the relay node, the sampled baseband signal is given by

$$y_r(k) = \sqrt{\frac{P_s}{d_1^m}} h s(k) + f x_r(k) + n_r(k), \quad (2)$$

where  $k$  denotes the symbol index,  $s(k)$  is the sampled and normalized information signal from the source,  $x_r(k)$  is the sampled signal of  $x_r(t)$ , and the second term on the right hand side is the loop interference. In this work, we do not investigate any self-interference cancellation schemes such that  $f$  may represent the loopback channel of the relay with or without self-interference cancellation. Using the harvested energy, the relay amplifies the received signal by a relay gain  $\beta$ . Then, the transmitted signal from the relay can be expressed as

$$x_r(k) = \sqrt{\beta} y_r(k - \tau), \quad (3)$$

where the integer  $\tau \geq 1$  is the processing delay at the relay. Recursive substitution of (2) and (3) shows that the transmitted signal from the relay can also be expressed as

$$x_r(k) = \sqrt{\beta} \sum_{j=1}^{\infty} (f \sqrt{\beta})^{j-1} \left( \sqrt{\frac{P_s}{d_1^m}} h s(k - j\tau) + n_r(k - j\tau) \right). \quad (4)$$

The sampled received signal at the destination is given by

$$y_d(k) = \frac{1}{\sqrt{d_2^m}} g x_r(k) + n_a^{[d]}(k) + n_c^{[d]}(k), \quad (5)$$

where  $d_2$  is the distance between the relay and the destination and  $n_a^{[d]}(k)$  and  $n_c^{[d]}(k)$  are the antenna and conversion AWGNs, respectively. The variances of  $n_a^{[d]}(k)$  and  $n_c^{[d]}(k)$  are  $\sigma_{n_a}^2$  and  $\sigma_{n_c}^2$ , respectively. Substituting (4) into (5), we have

$$y_d(k) = \sqrt{\frac{P_s \beta}{d_1^m d_2^m}} g h \sum_{j=1}^{\infty} (f \sqrt{\beta})^{j-1} s(k - j\tau) + \sqrt{\frac{\beta}{d_2^m}} g \sum_{j=1}^{\infty} (f \sqrt{\beta})^{j-1} n_r(k - j\tau) + n_d(k), \quad (6)$$

where  $n_d(k) \triangleq n_a^{[d]}(k) + n_c^{[d]}(k)$  is the zero mean AWGN at the destination node with variance  $\sigma_d^2 \triangleq \sigma_{n_a}^2 + \sigma_{n_c}^2$ .

We start studying the end-to-end signal power by deriving a condition to guarantee a non-oscillatory relay. By assuming all the signal and noise samples are mutually independent, the relay transmit power is calculated from (4) as

$$\begin{aligned} \mathbb{E}\{|x_r(k)|^2\} &= \beta \sum_{j=1}^{\infty} (|f|^2 \beta)^{j-1} ((d_1^m)^{-1} P_s |h|^2 + \sigma_r^2) \\ &= \beta \frac{(d_1^m)^{-1} P_s |h|^2 + \sigma_r^2}{1 - |f|^2 \beta}, \end{aligned} \quad (7)$$

where the relay gain must be limited by

$$\beta < \frac{1}{|f|^2}. \quad (8)$$

This condition prevents oscillation and guarantees finite relay transmit power. On the other hand, depending on the relay-harvested energy, the maximum relay transmit power is given by

$$P_r = \frac{E_h}{(1 - \alpha)T} = \frac{\mu P_s |h|^2}{d_1^m}, \quad (9)$$

where  $\mu \triangleq \frac{\alpha \eta}{1 - \alpha}$ . The actual relay transmit power should be less than or equal to the maximum relay transmit power, i.e.,

$$\mathbb{E}\{|x_r(k)|^2\} \leq P_r. \quad (10)$$

Substituting (7) and (9) into (10), the relay gain under the maximum relay transmit power is limited by

$$\beta \leq \frac{\mu}{1 + \gamma_{SR}^{-1} + \mu |f|^2}, \quad (11)$$

where the channel SNR of the first-hop link is defined as  $\gamma_{SR} \triangleq \frac{P_s |h|^2}{d_1^m \sigma_r^2}$ . At symbol index  $k$ , the destination node can employ any standard detection procedure to decode the desired signal



$s(k - \tau)$ , and the rest of the received signal components act as interference and noise. Again by requiring signal and noise independence, the received signal power at the destination is calculated from (5) as  $\mathbb{E}\{|y_d(k)|^2\} = (d_2^m)^{-1}g^2\mathbb{E}\{|x_r(k)|^2\} + \sigma_d^2$ . This expression with substitution of (7) can be further reorganized into a sum of desired signal power, loop interference power, and noise power, which can be expressed as

$$\begin{aligned} \mathbb{E}\{|y_d(k)|^2\} &= \underbrace{(d_1^m d_2^m)^{-1} P_s |h|^2 \beta |g|^2}_{\text{desired signal power}} + \underbrace{((d_1^m)^{-1} P_s |h|^2 + \sigma_r^2) \beta (d_2^m)^{-1} |g|^2 \frac{|f|^2 \beta}{1 - |f|^2 \beta}}_{\text{loop interference power}} \\ &\quad + \underbrace{\beta (d_2^m)^{-1} |g|^2 \sigma_r^2 + \sigma_d^2}_{\text{noise power}}. \end{aligned} \quad (12)$$

Using (12), the end-to-end SINR at the destination is given by

$$\gamma = \frac{\gamma_{\text{SR}} \gamma_{\text{RD}}}{\gamma_{\text{SR}}/\beta + \gamma_{\text{RD}} + (\gamma_{\text{SR}} + 1) \gamma_{\text{RD}} \frac{|f|^2}{1/\beta - |f|^2}}, \quad (13)$$

where the channel SNR of the second-hop link is defined as  $\gamma_{\text{RD}} \triangleq \frac{P_r}{\mu} \frac{|g|^2}{d_2^m \sigma_d^2} = \frac{P_s |h|^2 |g|^2}{d_1^m d_2^m \sigma_d^2}$ .

In this work, we consider that the systems work in the instantaneous transmission, the delay-limited transmission, and the delay-tolerant transmission modes, respectively. The system throughput of all the three transmission modes are, respectively, given by

$$R_{\text{I}}(\alpha, \beta) = (1 - \alpha) \log_2(1 + \gamma), \quad (14a)$$

$$R_{\text{DL}}(\alpha, \beta) = (1 - \alpha)(1 - P_{\text{out}})R, \quad (14b)$$

$$R_{\text{DT}}(\alpha, \beta) = (1 - \alpha)C_{\text{E}}, \quad (14c)$$

where  $P_{\text{out}} = \Pr(\gamma < \gamma_{\text{th}})$  is the outage probability,  $R = \log_2(1 + \gamma_{\text{th}})$  is the fixed transmit rate,  $C_{\text{E}} = \mathbb{E}\{\log_2(1 + \gamma)\}$  is the ergodic capacity, and  $\gamma_{\text{th}}$  is the threshold end-to-end SINR for correct data detection at the destination. The design goal of the relay control scheme is to maximize the system throughput by optimizing the control parameters  $\{\alpha, \beta\}$ . The optimal control parameters  $\{\alpha^*, \beta^*\}$  can be obtained by solving the following optimization problem

$$\begin{aligned} \{\alpha^*, \beta^*\} &= \arg \max_{\alpha, \beta} R_{\text{M}}(\alpha, \beta) \\ \text{subject to } & 0 < \alpha < 1 \quad \text{and} \quad 0 < \beta \leq \frac{\mu}{1 + \gamma_{\text{SR}}^{-1} + \mu |f|^2}, \end{aligned} \quad (15)$$

where  $R_{\text{M}}(\alpha, \beta)$  represents  $R_{\text{I}}(\alpha, \beta)$ ,  $R_{\text{DL}}(\alpha, \beta)$ , and  $R_{\text{DT}}(\alpha, \beta)$  for the instantaneous transmission, the delay-limited transmission, and the delay-tolerant transmission modes, respectively. For

the given expression of  $R_M(\alpha, \beta)$ , the optimal  $\{\alpha^*, \beta^*\}$  in (15) can be obtained by exhaustive searching all the possible combinations of  $\{\alpha, \beta\}$ .

In the following, all the three relay control schemes are presented, respectively. Then, the throughput performances are analyzed for all the three relay control schemes in the instantaneous transmission, the delay-limited transmission, and the delay-tolerant transmission modes, respectively.

### III. RELAY GAIN CONTROL

In this section, we discuss the three relay control schemes for selecting the relay gain and the TS factor. For the convenience of expression, each relay control scheme is named after the corresponding relay gain, e.g., the relay control scheme employing the maximum relay gain is called by the maximum relay gain, and so on.

#### A. The Maximum Relay Gain

A simple and popular relay control scheme is to set the relay gain with the maximum relay transmit power [27], [33]. The previous results of the maximum relay gain for wireless information and energy transfer can be found in [28]. In this work, we consider the maximum relay gain with main focus on its throughput performance in high INRs. For a given  $\alpha$  with any value in the range  $(0, 1)$ , the relay-harvested energy has a determined value and so does the maximum relay transmit power. According to (11), the maximum relay gain is given by

$$\beta_{\max} = \frac{\mu\gamma_{\text{SR}}}{1 + \gamma_{\text{SR}} + \mu\gamma_{\text{SR}}|f|^2}, \quad (16)$$

which guarantees that (8) holds. Substituting (16) into (13), the end-to-end SINR achieved by the maximum relay gain is given by

$$\gamma_{\max} = \frac{\mu\gamma_{\text{SR}}\gamma_{\text{RD}}}{\gamma_{\text{SR}} + (\mu\gamma_{\text{SR}}|f|^2 + 1)(\mu\gamma_{\text{RD}} + 1)}. \quad (17)$$

Since the relay can apply the maximum relay transmit power without knowing the actual CSI, the maximum relay gain is easy to realize. Note that both the maximum relay transmit power and the effective relaying transmission time are determined by TS, searching the optimal TS factor becomes critical for the system throughput maximization problem in (15). The optimized TS factor that maximizes the system throughput for all the three transmission modes will be discussed in the next section along with the throughput performance analysis.

### B. The Optimal Relay Gain

Without optimizing the TS factor, the maximum relay gain is not optimal in maximizing the end-to-end SINR, which in turn may have negative effect on the system throughput. Note that the system throughput is also determined by the relaying transmission time, the optimal relay gain is designed first to maximize the end-to-end SINR.

According to (12), considering the received signal power at the destination node as a function of the relay gain, the desired signal power is linear, but the loop interference power is nonlinear. Consequently, increasing the relay gain can increase the loop interference power faster than the desired signal power and lead to a reduced end-to-end SINR. It can be shown that (13) has a single maximum point for  $\beta \in (0, \frac{1}{|f|^2})$ . Thus, by setting the derivative of (13) equal to zero, the optimal relay gain, in terms of maximizing the end-to-end SINR, is obtained as

$$\beta_{\text{opt}} = \frac{\gamma_{\text{SR}}}{\gamma_{\text{SR}}|f|^2 + \sqrt{\gamma_{\text{SR}}(\gamma_{\text{SR}} + 1)\gamma_{\text{RD}}|f|^2}}, \quad (18)$$

which satisfies the non-oscillatory condition in (8). Substituting (18) into (13), the corresponding end-to-end SINR can be expressed as

$$\gamma_{\text{opt}} = \frac{\gamma_{\text{SR}}\gamma_{\text{RD}}}{\gamma_{\text{SR}}|f|^2 + \gamma_{\text{RD}} + 2\sqrt{\gamma_{\text{SR}}(\gamma_{\text{SR}} + 1)\gamma_{\text{RD}}|f|^2}}. \quad (19)$$

Obviously, the optimal relay gain should be designed with the full usage of the relay-harvested energy such that the relaying transmission time could be as long as possible. Therefore, by solving  $\beta_{\text{opt}} = \beta_{\text{max}}$  for any  $\alpha$  ( $0 < \alpha < 1$ ), the TS factor for the optimal relay gain is given by

$$\alpha_{\text{opt}} = \frac{\sqrt{\gamma_{\text{SR}} + 1}}{\sqrt{\gamma_{\text{SR}} + 1} + \eta\sqrt{\gamma_{\text{SR}}\gamma_{\text{RD}}|f|^2}}. \quad (20)$$

The TS factor  $\alpha_{\text{opt}}$  can be computed at the destination, or at the relay locally when the relay can access the global CSI. Note that no redundant energy has been harvested by employing  $\alpha_{\text{opt}}$ , the relaying transmission time  $(1 - \alpha_{\text{opt}})T$  is longer than that of any  $\alpha$  satisfying  $\alpha > \alpha_{\text{opt}}$ .

### C. The Target Relay Gain

When the optimal relay gain is employed, the knowledge of channel SNR  $\gamma_{\text{RD}}$  has to be exploited, which can be estimated only at the destination. A feedback channel is then required if  $\alpha_{\text{opt}}$  is computed locally at the relay. Therefore, a simplified relay control scheme that aims to achieve a target end-to-end SINR  $\hat{\gamma}$  is proposed. In order to avoid using the knowledge of

$\gamma_{\text{RD}}$ , the target end-to-end SINR should satisfy  $\hat{\gamma} < \gamma_{\text{SR}}$ . Denote the end-to-end SINR achieved by the target relay gain as  $\gamma_{\text{tar}}$  ( $\gamma_{\text{tar}} = \hat{\gamma}$ ), with the full usage of the maximum relay transmit power, the target relay gain is designed to make  $\gamma_{\text{tar}}$  optimal, i.e.,  $\gamma_{\text{tar}} = \gamma_{\text{opt}}$ . Denote the TS factor for the target relay gain by  $\alpha_{\text{tar}}$  and substitute  $\mu_{\text{tar}} \triangleq \frac{\alpha_{\text{tar}}\eta}{1-\alpha_{\text{tar}}}$  into (16) and (17), the target relay gain and the corresponding end-to-end SINR can be written as

$$\beta_{\text{tar}} = \frac{\mu_{\text{tar}}\gamma_{\text{SR}}}{1 + \gamma_{\text{SR}} + \mu_{\text{tar}}\gamma_{\text{SR}}|f|^2} \quad (21)$$

and

$$\gamma_{\text{tar}} = \frac{\mu_{\text{tar}}\gamma_{\text{SR}}\gamma_{\text{RD}}}{\gamma_{\text{SR}} + (\mu_{\text{tar}}\gamma_{\text{SR}}|f|^2 + 1)(\mu_{\text{tar}}\gamma_{\text{RD}} + 1)}, \quad (22)$$

respectively. For any given  $\hat{\gamma}$ , by eliminating  $\gamma_{\text{RD}}$  from the equation pair  $\{\gamma_{\text{tar}} = \hat{\gamma}, \gamma_{\text{opt}} = \hat{\gamma}\}$ , the TS factor is given by

$$\alpha_{\text{tar}} = \frac{(\gamma_{\text{SR}} + 1)(\gamma_{\text{SR}} - \hat{\gamma})}{(\gamma_{\text{SR}} + 1)(\gamma_{\text{SR}} - \hat{\gamma} + \eta\hat{\gamma}\gamma_{\text{SR}}|f|^2) + \eta\gamma_{\text{SR}}|f|^2\sqrt{\hat{\gamma}(\hat{\gamma} + 1)\gamma_{\text{SR}}(\gamma_{\text{SR}} + 1)}}. \quad (23)$$

Note that  $\hat{\gamma} < \gamma_{\text{SR}}$  also guarantees that  $0 < \alpha_{\text{tar}} < 1$ . When  $\hat{\gamma} \geq \gamma_{\text{SR}}$  happens, we have  $\alpha_{\text{tar}} \leq 0$ . In this case, no time is assigned for EH and the information relaying fails due to the lack of power. Alternatively, we can reset  $\hat{\gamma}$  such that  $\hat{\gamma} < \gamma_{\text{SR}}$  is satisfied, or we can reset the TS factor by  $\alpha_{\text{tar}} = 1$  such that EH is implemented for the whole time block.

#### IV. THROUGHPUT ANALYSIS

In this section, the throughput performances of the FDR systems are investigated for all the three relay control schemes in the instantaneous transmission, the delay-limited transmission, and the delay-tolerant transmission modes, respectively.

##### A. Instantaneous Transmission

When the optimal relay gain and the target relay gain are employed, the instantaneous throughput of the FDR system can be computed by using  $R_1 = (1 - \alpha)\log_2(1 + \gamma)$ , where  $\alpha$  is given by (20) and (23), respectively, and the end-to-end SINR is given by (19) and (22), respectively. For the optimal relay gain,  $\alpha_{\text{opt}}$  can be computed at the destination or the relay with the ideal global CSI assumption. For the target relay gain, since no knowledge of  $\gamma_{\text{RD}}$  is required, the TS factor can be calculated at the relay to reduce the feedback from the destination.

Note that when  $\hat{\gamma} \geq \gamma_{\text{SR}}$  happens, the instantaneous throughput achieved by the target relay gain is zero due to the failure of the effective relaying.

When the maximum relay gain is applied, the optimized TS factor can be obtained by solving the following optimization problem

$$\begin{aligned} \alpha^* &= \arg \max_{\alpha} R_I(\alpha) \\ \text{subject to } &0 < \alpha < 1. \end{aligned} \quad (24)$$

In (24),  $R_I(\alpha) = (1 - \alpha) \log_2(1 + \gamma_{\text{max}})$  is a concave function of  $\alpha$  and the optimized  $\alpha^*$  can be obtained by solving the equation  $\frac{dR_I(\alpha)}{d\alpha} = 0$ . However, due to the complicated expression of  $\frac{dR_I(\alpha)}{d\alpha} = 0$ , a closed-form solution is hardly possible and the online update of  $\alpha^*$  may be difficult for a device with limited computational capability. Similarly to [20], [28], this work obtains the optimized  $\alpha^*$  by using the build-in function "NSolve" of Mathematica.

### B. Delay-Limited Transmission

In the delay-limited transmission mode, the source transmits at a fixed rate  $R$  in order to meet some outage criteria. The average throughput is determined by  $R_{\text{DL}}(\alpha) = (1 - \alpha)(1 - P_{\text{out}})R$ .

*Proposition 1:* The outage probability achieved by the maximum relay gain is given by

$$P_{\text{out}} = 1 - \frac{1}{\lambda_f \lambda_h} \int_{w=0}^{\frac{1}{\mu \gamma_{\text{th}}}} \int_{z=\frac{d}{c}}^{\infty} e^{-\left(\frac{z}{\lambda_h} + \frac{az+b}{(cz^2-dz)\lambda_g}\right)} e^{-\frac{w}{\lambda_f}} dz dw \quad (25a)$$

$$\approx 1 - \frac{1}{\lambda_f} \int_0^{\frac{1}{\mu \gamma_{\text{th}}}} \rho K_1(\rho) e^{-\frac{d}{c\lambda_h} - \frac{w}{\lambda_f}} dw, \quad (\text{HSA}) \quad (25b)$$

where  $a \triangleq P_s d_1^m d_2^m \sigma_d^2 \gamma_{\text{th}} (1 + \mu w)$ ,  $b \triangleq d_1^{2m} d_2^m \sigma_r^2 \sigma_d^2 \gamma_{\text{th}}$ ,  $c \triangleq P_s \mu (1 - \mu \gamma_{\text{th}} w)$ ,  $d \triangleq P_s d_1^m \sigma_r^2 \mu \gamma_{\text{th}}$ ,  $\rho \triangleq \sqrt{\frac{4a}{c\lambda_g \lambda_h}}$ , and  $K_1(\cdot)$  is the first order modified Bessel function of the second kind [34, Eq. (8.432)].

*Proof:* See Appendix A. ■

Note that in (25b), the analytical expression is obtained by using high SINR approximation (HSA).

*Proposition 2:* The outage probability achieved by the optimal relay gain is given by

$$P_{\text{out}} = 1 - \frac{1}{\lambda_f \lambda_h} \int_0^{\infty} \left( \frac{az+b+c\sqrt{z(P_s z+d)}}{(P_s z - \gamma_{\text{th}} d)^2 \lambda_g} + \frac{1}{\lambda_f} \right)^{-1} e^{-\frac{z}{\lambda_h}} dz \quad (26a)$$

$$\approx 1 - e^{-\frac{v}{\lambda_h}} - \left(\rho + \frac{v}{\lambda_h}\right) e^{\rho} E_i(-\rho - \frac{v}{\lambda_h}), \quad (\text{HSA}) \quad (26b)$$

where  $a \triangleq P_s d_1^m d_2^m \sigma_d^2 \gamma_{\text{th}} (1 + 2\gamma_{\text{th}})$ ,  $b \triangleq d_1^{2m} d_2^m \sigma_r^2 \sigma_d^2 \gamma_{\text{th}}^2$ ,  $c \triangleq 2d_1^m d_2^m \sigma_d^2 \gamma_{\text{th}} \sqrt{P_s (1 + \gamma_{\text{th}}) \gamma_{\text{th}}}$ ,  $d \triangleq d_1^m \sigma_r^2$ ,  $v \triangleq \frac{2d_1^m \sigma_r^2 \gamma_{\text{th}}}{P_s}$ ,  $\rho \triangleq \frac{\lambda_f (a + c\sqrt{P_s}) - 2\lambda_g P_s d_1^m \sigma_r^2 \gamma_{\text{th}}}{\lambda_g \lambda_h P_s^2}$ , and  $E_i(\cdot)$  is the exponential integral function [34, Eq. (8.214)].

*Proof:* See Appendix B. ■

*Proposition 3:* The outage probability achieved by the target relay gain is given by

$$P_{\text{out}} = 1 - \frac{1}{\lambda_f \lambda_h} \int_{w=0}^{\infty} \int_{z=\hat{\gamma} d_1^m \sigma_r^2 / P_s}^{\infty} e^{-\frac{z}{\lambda_h} - \frac{w}{\lambda_f} + \frac{a q w}{(b z - c q)(d z + u - q v) \lambda_g}} dz dw \quad (27a)$$

$$\approx 1 - e^{-\frac{u}{(v\sqrt{P_s} - d)\lambda_h}} (1 + \omega e^{\omega} (\text{Chi}(\omega) - \text{Shi}(\omega))), \quad (\text{HSA}) \quad (27b)$$

where  $a \triangleq d_1^m d_2^m \sigma_d^2 \gamma_{\text{th}} \hat{\gamma} \sqrt{P_s \hat{\gamma} (1 + \hat{\gamma})}$ ,  $b \triangleq P_s \hat{\gamma} (1 + \gamma_{\text{th}})$ ,  $c \triangleq \gamma_{\text{th}} \sqrt{P_s \hat{\gamma} (1 + \hat{\gamma})}$ ,  $d \triangleq P_s \hat{\gamma}$ ,  $q \triangleq \sqrt{P_s z^2 + d_1^m \sigma_r^2 z}$ ,  $u \triangleq d_1^m \sigma_r^2 \hat{\gamma}$ ,  $v \triangleq \sqrt{P_s \hat{\gamma} (1 + \hat{\gamma})}$ ,  $\omega \triangleq \frac{a \sqrt{P_s} \lambda_f}{(b - c \sqrt{P_s})(v \sqrt{P_s} - d) \lambda_g \lambda_h}$ ,  $\text{Shi}(\cdot)$  and  $\text{Chi}(\cdot)$  are the hyperbolic sine integral function and the hyperbolic cosine integral function, respectively [34, Eq. (8.221)].

*Proof:* See Appendix C. ■

When the maximum relay gain is employed, the optimized TS factor can be obtained by solving

$$\begin{aligned} \alpha^* &= \arg \max_{\alpha} (1 - \alpha)(1 - P_{\text{out}})R \\ &\text{subject to } 0 < \alpha < 1. \end{aligned} \quad (28)$$

Due to the complicated expression of the derivative of  $(1 - \alpha)(1 - P_{\text{out}})R$ , the optimized  $\alpha^*$  is also obtained numerically. Since  $P_{\text{out}}$  in Proposition 1 contains only the statistic channel conditions, the instantaneous CSI has not been utilized to optimize the TS factor for the maximum relay gain.

In Proposition 2 and Proposition 3, although the TS factor doesn't appear in the expressions of  $P_{\text{out}}$ , the outage probabilities of the optimal relay gain and the target relay gain are derived with the pre-determined  $\alpha_{\text{opt}}$  and  $\alpha_{\text{tar}}$ , respectively. Moreover,  $\alpha_{\text{opt}}$  and  $\alpha_{\text{tar}}$  are computed with the instantaneous CSI. Thus, the average throughput of the FDR system for the optimal relay gain and the target relay gain can be evaluated by

$$R_{\text{DL}}(\bar{\alpha}) = (1 - \bar{\alpha})(1 - P_{\text{out}})R, \quad (29)$$

where  $\bar{\alpha} = \mathbb{E}\{\alpha_{\text{opt}}\}$  (or  $\bar{\alpha} = \mathbb{E}\{\alpha_{\text{tar}}\}$ ) when the optimal relay gain (or the target relay gain) is employed and the expectation value is obtained by the simulation. Since (29) involves both the

simulation of  $\bar{\alpha}$  and the analytical expression of  $P_{\text{out}}$ , it is a quasi-analytic method to evaluate the average throughput. Note that the relaying transmission fails for the target relay gain when  $\hat{\gamma} \geq \gamma_{\text{SR}}$  happens, the corresponding contribution to the average throughput should be set as zero.

### C. Delay-Tolerant Transmission

In the delay-tolerant transmission mode, the codeword length is very large compared to the channel block time such that the codeword could experience all possible realizations of the channel. Thus, the ergodic capacity becomes a measure determining the throughput performance and the source can transmit at any rate upper bounded by the ergodic capacity.

*Proposition 4:* The ergodic capacity achieved by the maximum relay gain is given by

$$C_E = \frac{1}{\ln 2} G_{4,2}^{1,4} \left( \frac{\mu P_s \lambda_g \lambda_h}{d_1^m d_2^m \sigma_d^2} \middle| \begin{matrix} 0,0,1,1 \\ 1,0 \end{matrix} \right) + \frac{1}{\ln 2} G_{4,2}^{1,4} \left( \frac{P_s \lambda_h (1+\lambda_f)}{d_1^m \sigma_r^2} \middle| \begin{matrix} 0,0,1,1 \\ 1,0 \end{matrix} \right) - \frac{1}{\lambda_h \lambda_g \lambda_f} \int_0^\infty \int_0^\infty \int_0^\infty e^{-\frac{z}{\lambda_h} - \frac{w}{\lambda_g} - \frac{v}{\lambda_f}} \xi(v, w, z) dz dw dv, \quad (30)$$

where  $\xi(v, w, z) = \log_2 \left( 1 + \frac{P_s z}{d_1^m \sigma_r^2} + \frac{\mu P_s z w}{d_1^m d_2^m \sigma_d^2} + \frac{\mu P_s z v}{d_1^m \sigma_r^2} + \frac{\mu^2 P_s^2 z^2 w v}{d_1^m d_2^m \sigma_r^2 \sigma_d^2} \right)$  and  $G_{m,n}^{p,q}(x)$  is the Meijer G-function [34, Eq. (9.301)].

*Proof:* See Appendix D. ■

The expression in Proposition 4 involves a triple integral. In order to facilitate further processing, the following upper bound on the ergodic capacity is presented.

*Corollary 1:* The ergodic capacity achieved by the maximum relay gain is upper bounded by

$$C_E^{\text{up}} = \frac{1}{\ln 2} G_{4,2}^{1,4} \left( \frac{\mu P_s \lambda_g \lambda_h}{d_1^m d_2^m \sigma_d^2} \middle| \begin{matrix} 0,0,1,1 \\ 1,0 \end{matrix} \right) + \frac{1}{\ln 2} G_{4,2}^{1,4} \left( \frac{P_s \lambda_h (1+\mu \lambda_h)}{d_1^m \sigma_r^2} \middle| \begin{matrix} 0,0,1,1 \\ 1,0 \end{matrix} \right) - \log_2 \left( 1 + \frac{P_s}{d_1^m \sigma_r^2} e^u + \frac{\mu P_s}{d_1^m d_2^m \sigma_d^2} e^v \right), \quad (31)$$

where  $u \triangleq \psi(1) + \ln \lambda_h + e^{\frac{1}{\mu \lambda_f}} \Gamma(0, \frac{1}{\mu \lambda_f})$ ,  $v \triangleq 2\psi(1) + \ln \lambda_g \lambda_h + G_{4,2}^{1,4} \left( \frac{\mu P_s \lambda_h \lambda_f}{d_1^m \sigma_r^2} \middle| \begin{matrix} 0,0,1,1 \\ 1,0 \end{matrix} \right)$ , and  $\psi(\cdot)$  is the digamma function [36, Eq.(8.360.1)].

*Proof:* Based on the fact that  $f(x, y) = \log_2(1 + e^x + e^y)$  is a convex function with respect to  $x$  and  $y$ , we have

$$\begin{aligned} & \mathbb{E}\{\log_2(1 + \gamma_{\text{SR}} + \mu \gamma_{\text{RD}} + \mu \gamma_{\text{SR}} |f|^2 + \mu^2 \gamma_{\text{SR}} \gamma_{\text{RD}} |f|^2)\} \\ &= \mathbb{E}\{\log_2(1 + \gamma_{\text{SR}}(1 + \mu |f|^2) + \mu \gamma_{\text{RD}}(1 + \mu \gamma_{\text{SR}} |f|^2))\} \\ &\geq \log_2 \left( 1 + \frac{P_s}{d_1^m \sigma_r^2} e^{\mathbb{E}\{\ln x\}} + \frac{\mu P_s}{d_1^m d_2^m \sigma_d^2} e^{\mathbb{E}\{\ln y\}} \right), \end{aligned} \quad (32)$$

where  $x \triangleq |h|^2(1 + \mu|f|^2)$  and  $y \triangleq |h|^2|g|^2(1 + \frac{\mu P_s}{d_1^m \sigma_r^2}|h|^2|f|^2)$ . With some mathematical manipulations, we have

$$\begin{aligned}\mathbb{E}\{\ln x\} &= \frac{1}{\lambda_f \lambda_h} \int_0^\infty \int_0^\infty e^{-\frac{z}{\lambda_h} - \frac{w}{\lambda_f}} \ln z(1 + \mu w) dz dw \\ &= \psi(1) + \ln \lambda_h + \frac{1}{\lambda_f} \int_0^\infty e^{-\frac{w}{\lambda_f}} \ln(1 + \mu w) dw \\ &= \psi(1) + \ln \lambda_h + e^{\frac{1}{\mu \lambda_f}} \Gamma(0, \frac{1}{\mu \lambda_f})\end{aligned}\quad (33)$$

and

$$\begin{aligned}\mathbb{E}\{\ln y\} &= \frac{1}{\lambda_f \lambda_g \lambda_h} \int_0^\infty \int_0^\infty \int_0^\infty e^{-\frac{w}{\lambda_f} - \frac{s}{\lambda_g} - \frac{z}{\lambda_h}} \ln z s (1 + \frac{\mu P_s}{d_1^m \sigma_r^2} z w) ds dz dw \\ &= 2\psi(1) + \ln \lambda_g \lambda_h + \frac{1}{\lambda_f \lambda_h} \int_0^\infty \int_0^\infty e^{-\frac{w}{\lambda_f} - \frac{z}{\lambda_h}} \ln(1 + \frac{\mu P_s}{d_1^m \sigma_r^2} z w) dz dw \\ &= 2\psi(1) + \ln \lambda_g \lambda_h + G_{4,2}^{1,4} \left( \frac{\mu P_s \lambda_h \lambda_f}{d_1^m \sigma_r^2} \middle| \begin{matrix} 0,0,1,1 \\ 1,0 \end{matrix} \right),\end{aligned}\quad (34)$$

which completes the proof. ■

*Proposition 5:* The ergodic capacity achieved by the optimal relay gain is given by

$$C_E = -\frac{1}{\lambda_f \lambda_h} \int_0^\infty \int_0^\infty \frac{\partial}{\partial \gamma} \left( \left( \frac{az+b+c\sqrt{z(P_s z+d)}}{(P_s z-\gamma d)^2 \lambda_g} + \frac{1}{\lambda_f} \right)^{-1} \right) e^{-\frac{z}{\lambda_h}} \log_2(1+\gamma) dz d\gamma \quad (35a)$$

$$\begin{aligned}\approx \int_0^\infty &\left( \frac{v}{\gamma \lambda_h} e^{-\frac{v}{\lambda_h}} - \tilde{a} e^{\rho-\omega} - \left( \tilde{b} \left( \rho + \frac{v}{\lambda_h} \right) e^{\frac{\rho}{P_s^2}} + \tilde{c} e^{\rho+\omega} \right) E_i \left( -\rho - \frac{v}{\lambda_h} \right) \right) \\ &\times \log_2(1+\gamma) d\gamma, \quad (\text{HSA}) \quad (35b)\end{aligned}$$

where  $a \triangleq P_s d_1^m d_2^m \sigma_d^2 \gamma (1+2\gamma)$ ,  $b \triangleq d_1^{2m} d_2^m \sigma_r^2 \sigma_d^2 \gamma^2$ , and  $c \triangleq 2 d_1^m d_2^m \sigma_d^2 \gamma \sqrt{P_s \gamma (1+\gamma)}$ , and  $d \triangleq d_1^m \sigma_r^2$ ,  $v = \frac{2 d_1^m \sigma_r^2 \gamma}{P_s}$ ,  $\tilde{a} \triangleq \frac{(1+\gamma+\sqrt{\gamma(1+\gamma)})(\lambda_h \rho + v)}{\lambda_h \gamma (1+\gamma)}$ ,  $\tilde{b} \triangleq -\frac{2d}{P_s \lambda_h} + \frac{\lambda_f}{P_s \lambda_h \lambda_g} \left( \frac{b(3+4\gamma)}{\gamma \sqrt{\gamma(1+\gamma)} \sigma_r^2} + d_1^m d_2^m (1+4\gamma) \sigma_d^2 \right)$ ,  $\tilde{c} \triangleq \frac{\lambda_f (2b\sqrt{P_s}(3+4\gamma)+c(1+4\gamma)\sigma_r^2)}{2P_s \lambda_h \lambda_g \gamma \sqrt{P_s \gamma (1+\gamma)} \sigma_r^2}$ ,  $\omega \triangleq \frac{(a+c\sqrt{P_s})\lambda_f}{P_s^4 \lambda_h \lambda_g}$ , and  $\rho = \frac{\lambda_f (a+c\sqrt{P_s})-2\lambda_g P_s d_1^m \sigma_r^2 \gamma}{\lambda_g \lambda_h P_s^2}$ .

*Proof:* See Appendix E. ■

Although the derivative in (35a) can be further expanded, it generates a very large expression, which cannot be handled easily. The following upper bound on the ergodic capacity is presented for further processing.

*Corollary 2:* The ergodic capacity achieved by the optimal relay gain is upper bounded by

$$C_E^{\text{up}} = \frac{1}{\ln 2} \left( \psi(1) + \ln \frac{P_s \lambda_h}{d_1^m \sigma_r^2} \right) - \log_2 \left( 1 + \frac{d_2^m \sigma_d^2}{\sigma_r^2} e^u + 2 \sqrt{\frac{d_2^m \sigma_d^2}{\sigma_r^2}} e^v \right), \quad (36)$$



where  $u = \ln \frac{\lambda_f}{\lambda_g}$  and  $v = \frac{1}{2} \left( e^{\frac{d_1^m \sigma_r^2}{P_s \lambda_h}} \Gamma(0, \frac{d_1^m \sigma_r^2}{P_s \lambda_h}) + \ln \frac{\lambda_f}{\lambda_g} \right)$ .

*Proof:* With the high SINR assumption, the ergodic capacity has the approximation of  $\mathbb{E}\{\log_2(1 + \gamma_{\text{opt}})\} \approx \mathbb{E}\{\log_2(\gamma_{\text{opt}})\}$ , which can be expressed by

$$\mathbb{E}\{\log_2(\gamma_{\text{opt}})\} = \mathbb{E}\{\log_2(\gamma_{\text{SR}})\} - \mathbb{E}\left\{\log_2\left(1 + \frac{\gamma_{\text{SR}}|f|^2}{\gamma_{\text{RD}}} + 2\sqrt{\frac{\gamma_{\text{SR}}(1+\gamma_{\text{SR}})|f|^2}{\gamma_{\text{RD}}}}\right)\right\}. \quad (37)$$

The first item can be evaluated as

$$\mathbb{E}\{\log_2(\gamma_{\text{SR}})\} = \frac{1}{\lambda_h} \int_0^\infty e^{-\frac{z}{\lambda_h}} \log_2\left(\frac{P_s z}{d_1^m \sigma_r^2}\right) dz = \frac{1}{\ln 2} \left( \psi(1) + \ln \frac{P_s \lambda_h}{d_1^m \sigma_r^2} \right). \quad (38)$$

According to the fact that  $f(x, y) = \log_2(1 + e^x + e^y)$  is a convex function with respect to  $x$  and  $y$ , the second item satisfies

$$\begin{aligned} & \mathbb{E}\left\{\log_2\left(1 + \frac{d_2^m \sigma_d^2}{\sigma_r^2} \frac{|f|^2}{|g|^2} + 2\sqrt{\frac{d_2^m \sigma_d^2}{\sigma_r^2}} \sqrt{\frac{|f|^2}{|g|^2}} \left(1 + \frac{P_s |h|^2}{d_1^m \sigma_r^2}\right)\right)\right\} \\ & \geq \log_2\left(1 + \frac{d_2^m \sigma_d^2}{\sigma_r^2} e^{\mathbb{E}\{\ln(|f|^2/|g|^2)\}} + 2\sqrt{\frac{d_2^m \sigma_d^2}{\sigma_r^2}} e^{\frac{1}{2}\mathbb{E}\left\{\ln\left(\frac{|f|^2}{|g|^2} \left(1 + \frac{P_s |h|^2}{d_1^m \sigma_r^2}\right)\right)\right\}}\right). \end{aligned} \quad (39)$$

With the help of the integration relationship [34, Eq. (4.352.1)], we have

$$\mathbb{E}\{\ln \frac{|f|^2}{|g|^2}\} = \frac{1}{\lambda_f \lambda_g} \int_0^\infty \int_0^\infty e^{-\frac{w}{\lambda_f} - \frac{z}{\lambda_g}} \ln \frac{w}{z} dz dw = \ln \frac{\lambda_f}{\lambda_g}. \quad (40)$$

Similarly, we get  $\mathbb{E}\left\{\ln\left(\frac{|f|^2}{|g|^2} \left(1 + \frac{P_s |h|^2}{d_1^m \sigma_r^2}\right)\right)\right\} = e^{\frac{d_1^m \sigma_r^2}{P_s \lambda_h}} \Gamma\left(0, \frac{d_1^m \sigma_r^2}{P_s \lambda_h}\right) + \ln \frac{\lambda_f}{\lambda_g}$ , which completes the proof.  $\blacksquare$

For the target relay gain, the effective EH and relaying transmission fail when  $\hat{\gamma} \geq \gamma_{\text{SR}}$  happens. In such case, the end-to-end SINR doesn't exist. Although the derivative of  $P_{\text{out}}$  in Proposition 3 can be obtained by mathematical manipulation, it cannot be used to represent the PDF of  $\gamma_{\text{tar}}$  due to the discontinuity. Therefore, it is difficult to evaluate  $\mathbb{E}\{\log_2(1 + \gamma_{\text{tar}})\}$  with the PDF of  $\gamma_{\text{tar}}$ . As an alternative, the ergodic capacity achieved by the target relay gain can be expressed by

$$C_E = \mathbb{E}\{\log_2(1 + \gamma_{\text{tar},1})\} - \mathbb{E}\{\log_2(1 + \gamma_{\text{tar},2})\}, \quad (41)$$

where  $\gamma_{\text{tar},1} \triangleq \frac{P_s x}{d_1^m d_2^m \hat{\gamma} \sigma_r^2 \sigma_d^2} + \frac{P_s^2(1+\hat{\gamma}-\sqrt{\hat{\gamma}(1+\hat{\gamma})})y}{d_1^m d_2^m \hat{\gamma} \sigma_r^2 \sigma_d^2}$ ,  $\gamma_{\text{tar},2} \triangleq \frac{P_s x}{d_1^m d_2^m \hat{\gamma} \sigma_r^2 \sigma_d^2} + \frac{P_s^2(1+2\hat{\gamma}-2\sqrt{\hat{\gamma}(1+\hat{\gamma})})y}{d_1^m d_2^m \hat{\gamma} \sigma_r^2 \sigma_d^2}$ ,  $x \triangleq \frac{|h|^2(a|g|^2+b|f|^2)}{|f|^2}$ ,  $y \triangleq \frac{|g|^2|h|^4}{|f|^2}$ ,  $a \triangleq (\sqrt{\hat{\gamma}(1+\hat{\gamma})} - \hat{\gamma})\sigma_r^2$ , and  $b \triangleq d_2^m \sigma_d^2 \sqrt{\hat{\gamma}(1+\hat{\gamma})}$ .

*Proposition 6:*  $\mathbb{E}\{\log_2(1 + \gamma_{\text{tar},1})\}$  and  $\mathbb{E}\{\log_2(1 + \gamma_{\text{tar},2})\}$  are, respectively, lower bounded by

$$\log_2 \left( 1 + \frac{P_s}{d_1^m d_2^m \hat{\gamma} \sigma_r^2 \sigma_d^2} e^u + \frac{P_s^2 (1 + \hat{\gamma} - \sqrt{\hat{\gamma}(1 + \hat{\gamma})})}{d_1^{2m} d_2^m \hat{\gamma} \sigma_r^2 \sigma_d^2} e^v \right) \quad (42)$$

and

$$\log_2 \left( 1 + \frac{P_s}{d_1^m d_2^m \hat{\gamma} \sigma_r^2 \sigma_d^2} e^u + \frac{P_s^2 (1 + 2\hat{\gamma} - 2\sqrt{\hat{\gamma}(1 + \hat{\gamma})})}{d_1^{2m} d_2^m \hat{\gamma} \sigma_r^2 \sigma_d^2} e^v \right), \quad (43)$$

where  $u \triangleq -E_i \left( -\frac{\hat{\gamma} d_1^m \sigma_r^2}{\lambda_h P_s} \right) + e^{-\frac{\hat{\gamma} d_1^m \sigma_r^2}{\lambda_h P_s}} \left( \frac{1}{a\lambda_g - b\lambda_f} a\lambda_g \ln \left( \frac{a\lambda_g}{b\lambda_f} \right) + \ln \left( \frac{b\hat{\gamma} d_1^m \sigma_r^2}{P_s} \right) \right)$  and  $v \triangleq -2E_i \left( -\frac{\hat{\gamma} d_1^m \sigma_r^2}{\lambda_h P_s} \right) - e^{-\frac{\hat{\gamma} d_1^m \sigma_r^2}{\lambda_h P_s}} \ln \left( \frac{\lambda_f P_s^2}{\lambda_g \hat{\gamma}^2 d_1^{2m} \sigma_r^4} \right)$ .

*Proof:* See Appendix F. ■

With the bounds in Proposition 6, the ergodic capacity achieved by the target relay gain can be approximated by

$$C_E \approx \log_2 \left( \frac{1 + \frac{P_s}{d_1^m d_2^m \hat{\gamma} \sigma_r^2 \sigma_d^2} e^u + \frac{P_s^2 (1 + \hat{\gamma} - \sqrt{\hat{\gamma}(1 + \hat{\gamma})})}{d_1^{2m} d_2^m \hat{\gamma} \sigma_r^2 \sigma_d^2} e^v}{1 + \frac{P_s}{d_1^m d_2^m \hat{\gamma} \sigma_r^2 \sigma_d^2} e^u + \frac{P_s^2 (1 + 2\hat{\gamma} - 2\sqrt{\hat{\gamma}(1 + \hat{\gamma})})}{d_1^{2m} d_2^m \hat{\gamma} \sigma_r^2 \sigma_d^2} e^v} \right). \quad (44)$$

Although the above expression is a rough bounded approximation, we will show lately that its changing trend is coincident with that of the simulation.

When the maximum relay gain is employed, the optimized  $\alpha^*$  can be obtained by solving the following problem

$$\begin{aligned} \alpha^* &= \arg \max_{\alpha} (1 - \alpha) C_E \\ &\text{subject to } 0 < \alpha < 1. \end{aligned} \quad (45)$$

Also, only statistic channel conditions are utilized in optimizing the TS factor for the maximum relay gain.

When the optimal relay gain and the target relay gain are employed, the quasi-analytic method is applied to evaluate the system throughput by

$$R_{\text{DT}}(\bar{\alpha}) = (1 - \bar{\alpha}) C_E, \quad (46)$$

where  $\bar{\alpha} = \mathbb{E}\{\alpha_{\text{opt}}\}$  (or  $\bar{\alpha} = \mathbb{E}\{\alpha_{\text{tar}}\}$ ) when the optimal relay gain (or the target relay gain) is employed and the expectation value is obtained by the simulation.

## V. NUMERICAL RESULTS

This section presents some numerical results to validate the analytical expressions developed in the previous section and discusses the performances for all the three relay control schemes. Unless otherwise stated, the source transmission rate is set to be  $R = 3$  bps/Hz and the corresponding outage SINR threshold is given by  $\gamma_{\text{th}} = 2^R - 1 = 7$ . The path loss exponent is set to be  $m = 3$ , while the distance  $d_1$  and  $d_2$  are normalized to unit value. The energy harvesting efficiency is set to be  $\eta = 0.4$ . The means of the dual-hop channel gains are set as  $\lambda_h = \lambda_g = 1$ . The source transmit SNR is defined as  $\text{SNR} \triangleq P_s/\sigma_r^2$ . For the loop interference channel, the instantaneous channel INR and the average channel INR are defined as  $\gamma_{\text{LI}} \triangleq \frac{|f|^2}{\sigma_r^2}$  and  $\bar{\gamma}_{\text{LI}} \triangleq \frac{\lambda_f}{\sigma_r^2}$ , respectively. For simplicity, similar noise variances at the relay and the destination nodes are assumed, i.e.,  $\sigma_r^2 = \sigma_d^2 = \sigma^2$ .

Fig. 2 deals with the impact of the TS factor on the instantaneous throughput. In Fig.2(a), we focus on a single frame with the following channel setting:  $|h|^2 = 1.898$ ,  $|g|^2 = 0.986$ ,  $|f|^2 = 1.3368$ . When SNR = 15 dB, 25 dB, and 35 dB, the target SINRs for the target relay gain are set by  $\hat{\gamma} = 8$  dB, 12 dB, and 14 dB, respectively. As can be readily observed, for all the three relay gains, the TS factor decreases when SNR increases. Although the optimal relay gain doesn't achieve the maximum throughput, its throughput is every close to the maximum throughput of the maximum relay gain. Besides, the target relay gain also achieves a competitive throughput. It also observed that  $\alpha_{\text{opt}}$  moves toward to the optimized  $\alpha^*$  when SNR increases. When SNR decreases, both  $\alpha_{\text{opt}}$  and the optimized  $\alpha^*$  increases, while  $\alpha_{\text{opt}}$  increases more quickly than the optimized  $\alpha^*$ . In such a case, the optimal relay gain results in a shorter relaying transmission time than that of the maximum relay gain employing the optimized  $\alpha^*$ . In Fig.2(b), we focus on a single frame with the following setting:  $|h|^2 = 1.898$ ,  $|g|^2 = 0.986$ ,  $|f|^2 = \gamma_{\text{LI}}\sigma_r^2$ , and SNR = 30 dB. The numerical results in Fig.2(b) also verify that a competitive throughput performance can be achieved by the optimal relay gain. Moreover,  $\alpha_{\text{opt}}$  decreases when  $\gamma_{\text{LI}}$  increases. This implies that a relatively long relaying transmission time is achieved for the optimal relay gain in high  $\gamma_{\text{LI}}$  range.

Fig. 3 illustrates the impacts of SNR and  $\gamma_{\text{LI}}$  on the instantaneous throughput. In Fig. 3(a), we set SNR = 35 dB and  $\hat{\gamma} = 22$ . It can be observed in Fig. 3(a) that the optimal relay gain achieves the same throughput as that of the maximum relay gain in the high  $\gamma_{\text{LI}}$  range. When

$\gamma_{\text{LI}}$  has the low values, the throughput performance of the optimal relay gain is worse than that of the maximum relay gain. This phenomenon is coincident with the fact that  $(1 - \alpha_{\text{opt}})T$  becomes small when  $\gamma_{\text{LI}}$  decreases, as previously shown in Fig. 2(b). Fig. 3(a) also shows that the throughput of the target relay gain can not only catch up but also surpass that of the optimal relay gain. This suggests that the target relay gain is more suitable than the optimal relay in the scenario where the channel SNR  $\gamma_{\text{RD}}$  is not available. The curves of instantaneous throughput versus SNR are plotted in Fig. 3(b), where we fixed  $\gamma_{\text{LI}} = 35$  dB. In the whole SNRs, the optimal relay gain achieves almost the same throughput as that of the maximum relay gain. Since the optimized  $\alpha^*$  is numerically obtained while  $\alpha_{\text{opt}}$  has the closed-form expression, the optimal relay gain is more preferable than the maximum relay gain in the high  $\gamma_{\text{LI}}$  range for all SNRs.

Fig. 4 investigates the impact of  $\hat{\gamma}$  on the instantaneous throughput for the target relay gain. The two-hop channel gains are set by  $|h|^2 = 1.898$  and  $|g|^2 = 0.986$ , while the loop interference channel is set by  $|f|^2 = \gamma_{\text{LI}}\sigma_r^2$ . As can be seen in Fig. 4, the maximum throughputs of the target relay gain are always achieved with the target SINRs satisfying  $\hat{\gamma} < \gamma_{\text{SR}}$ . For example, when SNR = 35 dB and  $\gamma_{\text{LI}} = 25$  dB, the channel SNR of the first-hop link is  $\gamma_{\text{SR}} = 37.78$  dB, while the target SINR achieving the maximum throughput is  $\hat{\gamma} = 23$  dB, which satisfies  $\hat{\gamma} < \gamma_{\text{SR}}$ . However, about 2 bps/Hz throughput decreasing happens when  $\hat{\gamma}$  moves about 7.5 dB away from  $\hat{\gamma} = 23$  dB. Thus, the target relay gain is not suitable for the scenario where the priority is throughput maximization.

Fig. 5 examines the analytical results for the outage probability versus SNR. In the simulation, 20,000 random channel realizations have been applied. Both the analytical and the analytical approximation (defined in figure as "Anal. Approx.") expressions for the outage probability are evaluated. It can be observed from Fig. 5 that the analytical and the simulation results match in all SNRs with the fixed  $\bar{\gamma}_{\text{LI}}$ . The results verifies the analytical expression for  $P_{\text{out}}$  presented in Proposition 1, 2, and 3, respectively. Fig. 5 also shows that the optimal relay gain always has an equal or lower outage probability than the maximum relay gain, while the target relay gain achieves a better outage probability performance than the maximum relay gain in high SNRs. The reason is that a higher SNR results in a higher  $\gamma_{\text{SR}}$ , which in turn leads to a larger upper bound of  $\hat{\gamma}$  (note that  $\hat{\gamma} < \gamma_{\text{SR}}$  is required to implement the target relay gain).

Fig. 6 deals with the analytical results for the outage probability versus  $\bar{\gamma}_{\text{LI}}$ . For the target relay

gain, the target SINR is set as  $\hat{\gamma} = 8$  dB. In the high  $\bar{\gamma}_{\text{LI}}$  range, the analytical and simulation results for all the relay control schemes match well. However, In the low  $\bar{\gamma}_{\text{LI}}$  range, the deviation between the analytical and simulation results happens for the optimal relay gain and the target relay gain, respectively. In practice, the FDR systems in most cases have to face a high level of loop interference, which validates the effectiveness of applying the derived analytical expressions.

Fig. 7 examines the analytical results for the ergodic capacity versus SNR. For the target relay gain, the target SINR is set as  $\hat{\gamma} = 15$  dB. For  $C_E$  of the maximum relay gain and the optimal relay gain, the analytical expressions and the simulation results match well. Fig. 7 also verifies the effectiveness of the  $C_E$  upper bound for the maximum relay gain. For  $C_E$  of the target relay gain, although the bounded approximation and the simulation results have a deviation, their changing trends are coincident. It can be observed that the ergodic capacity achieved by the optimal relay gain is higher than that of the maximum relay gain, while the ergodic capacity achieved by the target relay gain is higher than that of the maximum relay around the target ergodic capacity. For example, the target ergodic capacity is  $\mathbb{E}\{\log_2(1 + \hat{\gamma})\} \approx 5.03$  bps/Hz when  $\hat{\gamma} = 15$  dB (linear  $\hat{\gamma} \approx 31.62$ ). As can be observed, when the ergodic capacity is 5.03 bps/Hz and  $\bar{\gamma}_{\text{LI}} = 15$  dB, the target relay gain achieves about 6 dB SNR gain when compared with the maximum relay gain.

Fig. 8 examines the ergodic capacity versus  $\bar{\gamma}_{\text{LI}}$ . For the target relay gain, the target SINR is set as  $\hat{\gamma} = 8$  dB. As can be observed, the analytical expressions and the simulation results match well and the achieved ergodic capacities for all the relay gains decrease when  $\bar{\gamma}_{\text{LI}}$  increases. Although the  $C_E$  upper bound for the maximum relay gain is higher than  $C_E$  for the optimal relay gain in the high  $\bar{\gamma}_{\text{LI}}$  range,  $C_E$  for the maximum relay gain is always lower than that of the optimal relay gain. The reason is that the end-to-end SINR for the maximum relay is always smaller than that of the optimal relay gain. Similar to Fig. 7, Fig. 8 also shows that the bounded approximation of  $C_E$  for the target relay gain can not match well with the simulation result, while their changing trends are coincident.

Fig. 9 illustrates the throughput of different scenarios. In the evaluation of Fig. 9, we set  $\bar{\gamma}_{\text{LI}} = 45$  dB and  $\hat{\gamma} = 22$  dB. As can be observed, the throughput in the instantaneous transmission mode is the largest and both the maximum relay gain and optimal relay gain achieve the largest throughput. Due to its closed-form TS factor, the optimal relay gain appears to be more preferable than the maximum relay gain. It can be observed that the optimal relay gain in the delay-tolerant

transmission mode also achieves the largest throughput, while the maximum relay gain and the target relay gain do not. Fig. 9 also shows that the throughput for the target relay gain is larger than that for the maximum relay gain in certain SNRs. As expected, the throughput in the delay-limited transmission mode is upper bounded by the constant transmission rate  $R = 3$  bps/Hz. Moreover, we observe that in the delay-limited scenario, the throughput for the optimal relay gain is larger than that for the maximum relay gain.

The curves of throughput versus  $\bar{\gamma}_{\text{LI}}$  for all the three relay control schemes in the delay-limited and the delay-tolerant transmission modes are plotted in Fig. 10, where we set  $\text{SNR} = 35$  dB and  $\hat{\gamma} = 15$  dB. As can be readily observed, the throughput for the optimal relay gain is larger than that for the maximum relay gain in the high  $\bar{\gamma}_{\text{LI}}$  range. However, in the low  $\bar{\gamma}_{\text{LI}}$  range, the throughput for the optimal relay gain is lower than that for the maximum relay gain. Although the optimal relay gain achieves the better performances of the outage probability and the ergodic capacity, the throughput is meanwhile affected by the relaying transmission time  $(1 - \alpha)T$ . Recall from Fig. 2(b) that  $\alpha_{\text{opt}}$  is larger than  $\alpha^*$ , it can be concluded that the relaying transmission time for the optimal relay gain becomes smaller than that for the maximum relay gain. This explains that why the optimal relay gain achieves a lower throughput in the low  $\bar{\gamma}_{\text{LI}}$  range. Fig. 10 also shows that the largest throughput achieved by the target relay gain is competitive to that of the maximum relay gain. Since a small  $\alpha_{\text{tar}}$  can be obtained with high SNR and  $\bar{\gamma}_{\text{LI}}$  (recall the results in Fig. 2), an interested target throughput could be obtained by tuning the target SINR  $\hat{\gamma}$ .

Fig. 11 illustrates the throughput performance versus the relay location. In the evaluation, we set  $\text{SNR} = 50$  dB,  $\bar{\gamma}_{\text{LI}} = 35$  dB,  $d_1 + d_2 = 2$ , and  $d_1$  varies from 0.1 to 0.9. It can be observed from Fig. 11(a) that, in the delay-tolerant transmission mode, the throughputs for the maximum relay gain and the optimal relay gain firstly decrease and then increase with the growth of  $d_1$ . For the maximum relay gain and the optimal relay gain, the lowest throughput is achieved when the relay is placed in the middle of the source and the destination. The reason is that the maximum end-to-end SINR can be achieved only when the channel SNRs of the first and the second hops are balanced, i.e., the distances  $d_1$  and  $d_2$  are equal. When the maximum relay gain and the optimal relay gain are employed, for two relay nodes whose positions are symmetric about the middle of the source and the destination, the throughput of the relay near the source is higher than that of the relay near the destination. The reason is that the farther the distance between

the source and the relay, the less the relay-harvested energy due to the path loss effect. When the target SINR is quite smaller than  $\gamma_{\text{SR}}$ , the throughput achieved by the target relay gain is a constant for different  $d_1$ . The reason of this scenario is that  $\gamma_{\text{SR}}$  is high enough such that  $\gamma_{\text{tar}} = \hat{\gamma}$  can be exactly achieved with sufficient EH even for different  $d_1$ . However, when  $\hat{\gamma}$  becomes high, a long distance  $d_1$  results in insufficient EH and the throughput decreases. For a high  $\hat{\gamma}$  closer to  $\gamma_{\text{SR}}$ , the throughput for the target relay gain decreases dramatically. The results in Fig. 11(b) also verifies that the throughput for the target relay gain decreases dramatically for the high  $\hat{\gamma}$  when the relay moves from the source towards the destination. For the maximum relay gain and the optimal relay in the delay-limited transmission mode, the relative worse throughput performances are also achieved by the relay located in the middle of the source and the relay. Similar phenomena happen for all the three relay control schemes in the instantaneous transmission mode and the results are omitted here.

## VI. CONCLUSION

This paper studied the wireless information and energy transfer for the AF FDR systems, where the unavoidable high loop interference degrades the system performance. Three relay control schemes, namely, the maximum relay gain, the optimal relay, and the target relay gain were investigated in the different transmission modes, respectively. Analytical expressions for the outage probability and the ergodic capacity were derived for all the three relay control schemes in the delay-limited and the delay-tolerant transmission modes, respectively. For the optimal relay gain and the target relay gain, the TS factors were presented in closed-form in terms of the instantaneous CSI. Various numerical results were presented to confirm our analytical results and to reveal the impacts of relay control schemes on the system performance. It is shown that the optimal relay gain achieves the better performance of the outage probability and the ergodic capacity than that of the maximum relay gain, while the target relay gain achieves the competitive throughput performance without requiring the CSI of the second-hop link. The numerical results also illustrated that the relative worse throughput performance for the maximum relay gain and the optimal relay is achieved by the relay located in the middle between the source and the destination, while the throughput for the target relay gain with the high target SINR decreases dramatically when the relay moves from the source towards the destination.



## APPENDIX A

This part derives the outage probability achieved by the maximum relay gain  $\beta_{\max}$ . Substituting (17) into  $P_{\text{out}} = \Pr(\gamma_{\max} < \gamma_{\text{th}})$ , the outage probability is given by

$$\begin{aligned} P_{\text{out}} &= \Pr\left(\frac{\mu\gamma_{\text{SR}}\gamma_{\text{RD}}}{\gamma_{\text{SR}} + (\mu\gamma_{\text{SR}}|f|^2 + 1)(\mu\gamma_{\text{RD}} + 1)} < \gamma_{\text{th}}\right) \\ &= \Pr\left(|g|^2 < \frac{P_s d_1^m d_2^m \sigma_d^2 \gamma_{\text{th}} (1 + \mu|f|^2) |h|^2 + d_1^{2m} d_2^m \sigma_r^2 \sigma_d^2 \gamma_{\text{th}}}{P_s^2 \mu (1 - \mu\gamma_{\text{th}}|f|^2) |h|^4 - P_s d_1^m \sigma_r^2 \mu\gamma_{\text{th}} |h|^2}\right) \\ &= \Pr\left(|g|^2 < \frac{\bar{a}|h|^2 + b}{\bar{c}|h|^4 - d|h|^2}\right), \end{aligned} \quad (\text{A.1})$$

where  $\bar{a} \triangleq P_s d_1^m d_2^m \sigma_d^2 \gamma_{\text{th}} (1 + \mu|f|^2)$ ,  $b \triangleq d_1^{2m} d_2^m \sigma_r^2 \sigma_d^2 \gamma_{\text{th}}$ ,  $\bar{c} \triangleq P_s^2 \mu (1 - \mu\gamma_{\text{th}}|f|^2)$ , and  $d \triangleq P_s d_1^m \sigma_r^2 \mu\gamma_{\text{th}}$ . Since the term  $\bar{c}|h|^4 - d|h|^2$  can be positive or negative and  $|g|^2$  is always greater than a negative number,  $P_{\text{out}}$  can be simplified as

$$P_{\text{out}} = \begin{cases} \Pr\left(|g|^2 < \frac{\bar{a}|h|^2 + b}{\bar{c}|h|^4 - d|h|^2}\right), & |f|^2 < \frac{1}{\mu\gamma_{\text{th}}} \text{ and } |h|^2 > \frac{d}{c} \\ 1, & |f|^2 < \frac{1}{\mu\gamma_{\text{th}}} \text{ and } |h|^2 < \frac{d}{c} \\ 1, & |f|^2 > \frac{1}{\mu\gamma_{\text{th}}} \text{ and } |h|^2 > 0 \end{cases} \quad (\text{A.2})$$

Denote the probability density functions (PDFs) of the exponential random variable  $|h|^2$  and  $|f|^2$  by  $f_{|h|^2}(z) \triangleq \frac{1}{\lambda_h} e^{-\frac{z}{\lambda_h}}$  and  $f_{|f|^2}(z) \triangleq \frac{1}{\lambda_f} e^{-\frac{z}{\lambda_f}}$ , respectively, where  $\lambda_h$  and  $\lambda_f$  are the means of  $|h|^2$  and  $|f|^2$ , respectively. Denote the cumulative distribution function (CDF) of the exponential random variable  $|g|^2$  by  $F_{|g|^2}(z) \triangleq \Pr(|g|^2 < z) = 1 - e^{-\frac{z}{\lambda_g}}$ , where  $\lambda_g$  is the mean of  $|g|^2$ .

Following (A.2),  $P_{\text{out}}$  is given by

$$\begin{aligned} P_{\text{out}} &= \int_{w=\frac{1}{\mu\gamma_{\text{th}}}}^{\infty} \int_{z=0}^{\infty} f_{|f|^2}(w) f_{|h|^2}(z) dz dw + \int_{w=0}^{\frac{1}{\mu\gamma_{\text{th}}}} \int_{z=0}^{\frac{d}{c}} f_{|h|^2}(z) f_{|f|^2}(w) dz dw \\ &\quad + \int_{w=0}^{\frac{1}{\mu\gamma_{\text{th}}}} \int_{z=\frac{d}{c}}^{\infty} f_{|h|^2}(z) f_{|f|^2}(w) \Pr\left(|g|^2 < \frac{az+b}{cz^2-dz}\right) dz dw \\ &= e^{-\frac{1}{\mu\gamma_{\text{th}}\lambda_f}} + \frac{1}{\lambda_f} \int_{w=0}^{\frac{1}{\mu\gamma_{\text{th}}}} \left( \int_{z=0}^{\frac{d}{c}} f_{|h|^2}(z) dz + \int_{z=\frac{d}{c}}^{\infty} f_{|h|^2}(z) \left(1 - e^{-\frac{az+b}{(cz^2-dz)\lambda_g}}\right) dz \right) e^{-\frac{w}{\lambda_f}} dw \\ &= 1 - \frac{1}{\lambda_f \lambda_h} \int_{w=0}^{\frac{1}{\mu\gamma_{\text{th}}}} \int_{z=\frac{d}{c}}^{\infty} e^{-\left(\frac{z}{\lambda_h} + \frac{az+b}{(cz^2-dz)\lambda_g}\right)} e^{-\frac{w}{\lambda_f}} dz dw, \end{aligned} \quad (\text{A.3})$$

where  $a \triangleq P_s d_1^m d_2^m \sigma_d^2 \gamma_{\text{th}} (1 + \mu w)$  and  $c \triangleq P_s^2 \mu (1 - \mu\gamma_{\text{th}} w)$ . The analytical expression of  $P_{\text{out}}$  in (A.3) cannot be further simplified. However, at high SINR,  $\frac{az+b}{cz^2-dz}$  has the approximation  $\frac{a}{cz-d}$ . Thus, with high SINR approximation,  $P_{\text{out}}$  in (A.3) can be approximated as



$$\begin{aligned}
P_{\text{out}} &\approx 1 - \frac{1}{\lambda_f \lambda_h} \int_{w=0}^{\frac{1}{\mu \gamma_{\text{th}}}} \int_{z=\frac{d}{c}}^{\infty} e^{-\left(\frac{z}{\lambda_h} + \frac{a}{(cz-d)\lambda_g}\right)} e^{-\frac{w}{\lambda_f}} dz dw \\
&\stackrel{x \triangleq cz-d}{=} 1 - \frac{1}{c \lambda_f \lambda_h} \int_{w=0}^{\frac{1}{\mu \gamma_{\text{th}}}} \int_{x=0}^{\infty} e^{-\left(\frac{x}{c \lambda_h} + \frac{a}{x \lambda_g}\right)} e^{-\frac{d}{c \lambda_h}} e^{-\frac{w}{\lambda_f}} dx dw \\
&= 1 - \frac{1}{\lambda_f} \int_0^{\frac{1}{\mu \gamma_{\text{th}}}} \rho K_1(\rho) e^{-\frac{d}{c \lambda_h} - \frac{w}{\lambda_f}} dw,
\end{aligned} \tag{A.4}$$

where  $\rho \triangleq \sqrt{\frac{4a}{c \lambda_h \lambda_g}}$  and  $K_1(\cdot)$  is the first-order modified Bessel function of the second kind [34, Eq. (8.432)]. The last equality in (A.4) is obtained by applying  $\int_0^\infty e^{-\frac{\alpha}{4x} - \beta x} dx = \sqrt{\frac{\alpha}{\beta}} K_1(\sqrt{\alpha \beta})$  [34, Eq. (3.324.1)].

## APPENDIX B

This part derives the outage probability achieved by the optimal relay gain. Substituting (19) into  $P_{\text{out}} = \Pr(\gamma_{\text{opt}} < \gamma_{\text{th}})$ , the outage probability is given by

$$\begin{aligned}
P_{\text{out}} &= \Pr\left(\frac{\gamma_{\text{SR}} \gamma_{\text{RD}}}{\gamma_{\text{SR}} |f|^2 + \gamma_{\text{RD}} + 2\sqrt{\gamma_{\text{SR}}(\gamma_{\text{SR}}+1)\gamma_{\text{RD}}|f|^2}} < \gamma_{\text{th}}\right) \\
&= \Pr\left(|g|^2 < \frac{P_s |f|^2 d_1^m d_2^m \sigma_d^2 \gamma_{\text{th}} (1+2\gamma_{\text{th}}) |h|^2 + |f|^2 d_1^{2m} d_2^m \sigma_r^2 \sigma_d^2 \gamma_{\text{th}}^2}{P_s^2 |h|^4 - 2P_s d_1^m \sigma_r^2 \gamma_{\text{th}} |h|^2 + d_1^{2m} \sigma_r^4 \gamma_{\text{th}}^2} \right. \\
&\quad \left. + \frac{2|f|^2 d_1^m d_2^m \sigma_d^2 \gamma_{\text{th}} \sqrt{P_s(1+\gamma_{\text{th}})\gamma_{\text{th}}} \sqrt{|h|^2(P_s|h|^2 + d_1^m \sigma_r^2)}}{P_s^2 |h|^4 - 2P_s d_1^m \sigma_r^2 \gamma_{\text{th}} |h|^2 + d_1^{2m} \sigma_r^4 \gamma_{\text{th}}^2}\right) \\
&= \Pr\left(|g|^2 < \frac{\bar{a}|h|^2 + \bar{b} + \bar{c} \sqrt{|h|^2(P_s|h|^2 + d)}}{(P_s|h|^2 - \gamma_{\text{th}} d)^2}\right),
\end{aligned} \tag{B.1}$$

where  $\bar{a} \triangleq P_s |f|^2 d_1^m d_2^m \sigma_d^2 \gamma_{\text{th}} (1+2\gamma_{\text{th}})$ ,  $\bar{b} \triangleq |f|^2 d_1^{2m} d_2^m \sigma_r^2 \sigma_d^2 \gamma_{\text{th}}^2$ ,  $\bar{c} = 2|f|^2 d_1^m d_2^m \sigma_d^2 \gamma_{\text{th}} \sqrt{P_s(1+\gamma_{\text{th}})\gamma_{\text{th}}}$ , and  $d \triangleq d_1^m \sigma_r^2$ . Substituting  $f_{|h|^2}(z) \triangleq \frac{1}{\lambda_h} e^{-\frac{z}{\lambda_h}}$ ,  $f_{|f|^2}(z) \triangleq \frac{1}{\lambda_f} e^{-\frac{z}{\lambda_f}}$ , and  $F_{|g|^2}(z) \triangleq \Pr(|g|^2 < z) = 1 - e^{-\frac{z}{\lambda_g}}$  into (B.1), the outage probability can be written as

$$\begin{aligned}
P_{\text{out}} &= \int_0^\infty \int_0^\infty f_{|f|^2}(w) f_{|h|^2}(z) \Pr\left(|g|^2 < \frac{\bar{a}z + \bar{b} + \bar{c} \sqrt{z(P_s z + d)}}{(P_s z - \gamma_{\text{th}} d)^2}\right) dz dw \\
&= 1 - \frac{1}{\lambda_f \lambda_h} \int_0^\infty \int_0^\infty e^{-\frac{z}{\lambda_h} - \frac{w \left( \frac{\bar{a}z + \bar{b} + \bar{c} \sqrt{z(P_s z + d)}}{(P_s z - \gamma_{\text{th}} d)^2} \lambda_g \right)}{ \lambda_f}} dz dw \\
&= 1 - \frac{1}{\lambda_f \lambda_h} \int_0^\infty \left( \frac{\bar{a}z + \bar{b} + \bar{c} \sqrt{z(P_s z + d)}}{(P_s z - \gamma_{\text{th}} d)^2 \lambda_g} + \frac{1}{\lambda_f} \right)^{-1} e^{-\frac{z}{\lambda_h}} dz,
\end{aligned} \tag{B.2}$$

where  $a \triangleq P_s d_1^m d_2^m \sigma_d^2 \gamma_{\text{th}} (1 + 2\gamma_{\text{th}})$ ,  $b \triangleq d_1^{2m} d_2^m \sigma_r^2 \sigma_d^2 \gamma_{\text{th}}^2$ , and  $c \triangleq 2d_1^m d_2^m \sigma_d^2 \gamma_{\text{th}} \sqrt{P_s(1 + \gamma_{\text{th}})\gamma_{\text{th}}}$ . The expression in (B.2) cannot be further simplified. However, high SINR approximation can be applied to simplify the expression. At high SINR, the terms  $\bar{b}$ ,  $\bar{c}\sqrt{|h|^2(P_s|h|^2 + d)}$ , and  $(P_s|h|^2 - \gamma_{\text{th}}d)^2$  in (B.2) can be approximated by  $\bar{b} \approx 0$ ,  $\bar{c}\sqrt{|h|^2(P_s|h|^2 + d)} \approx \bar{c}\sqrt{P_s}|h|^2$ , and  $(P_s|h|^2 - \gamma_{\text{th}}d)^2 \approx P_s^2|h|^4 - u|h|^2$ , respectively, where  $u \triangleq 2P_s d_1^m \sigma_r^2 \gamma_{\text{th}}$ . Thus,  $P_{\text{out}}$  in (B.1) can be approximated by

$$P_{\text{out}} \approx \begin{cases} \Pr\left(|g|^2 < \frac{\bar{a} + \bar{c}\sqrt{P_s}}{P_s^2|h|^2 - u}\right), & |h|^2 > \frac{2d_1^m \sigma_r^2 \gamma_{\text{th}}}{P_s} \\ 1, & |h|^2 < \frac{2d_1^m \sigma_r^2 \gamma_{\text{th}}}{P_s} \end{cases} \quad (\text{B.3})$$

Following (B.3), after some mathematical manipulation,  $P_{\text{out}}$  can be written as

$$\begin{aligned} P_{\text{out}} &\approx \int_0^\infty \int_0^{\frac{2d_1^m \sigma_r^2 \gamma_{\text{th}}}{P_s}} f_{|f|^2}(w) f_{|h|^2}(z) dz dw \\ &\quad + \int_0^\infty \int_{\frac{2d_1^m \sigma_r^2 \gamma_{\text{th}}}{P_s}}^\infty f_{|f|^2}(w) f_{|h|^2}(z) \Pr\left(|g|^2 < \frac{\bar{a} + \bar{c}\sqrt{P_s}}{P_s^2|h|^2 - u}\right) dz dw \\ &= 1 - \frac{1}{\lambda_f \lambda_h} \int_{\frac{2d_1^m \sigma_r^2 \gamma_{\text{th}}}{P_s}}^\infty \left( \frac{a + c\sqrt{P_s}}{(P_s^2 z - u)\lambda_g} + \frac{1}{\lambda_f} \right)^{-1} e^{-\frac{z}{\lambda_h}} dz \\ &= 1 - e^{-\frac{v}{\lambda_h}} - \left( \rho + \frac{u}{\lambda_h P_s^2} \right) e^\rho E_i(-\rho - \frac{v}{\lambda_h}), \end{aligned} \quad (\text{B.4})$$

where  $\rho = \frac{\lambda_f(a + c\sqrt{P_s}) - \lambda_g u}{\lambda_g \lambda_h P_s^2}$ ,  $v = \frac{2d_1^m \sigma_r^2 \gamma_{\text{th}}}{P_s}$ , and  $E_i(\cdot)$  is the exponential integral function [34, Eq. (8.214)].

## APPENDIX C

This part derives the outage probability achieved by the target relay gain. Given  $\gamma_{\text{tar}}$  in (22) and  $\alpha_{\text{tar}}$  in (23), the outage probability is given by

$$\begin{aligned} P_{\text{out}} &= \Pr\left(\frac{\mu_{\text{tar}} \gamma_{\text{SR}} \bar{\gamma}_{\text{RD}}}{\gamma_{\text{SR}} + (\mu_{\text{tar}} \gamma_{\text{SR}} |f|^2 + 1)(\mu_{\text{tar}} \bar{\gamma}_{\text{RD}} + 1)} < \gamma_{\text{th}}\right) \\ &= \Pr\left(|g|^2 < -\frac{a\tilde{q}|f|^2}{(b|h|^2 - c\tilde{q})(d|h|^2 + u - v\tilde{q})}\right), \end{aligned} \quad (\text{C.1})$$

where  $a \triangleq d_1^m d_2^m \sigma_d^2 \gamma_{\text{th}} \hat{\gamma} \sqrt{P_s \hat{\gamma} (1 + \hat{\gamma})}$ ,  $b \triangleq P_s \hat{\gamma} (1 + \gamma_{\text{th}})$ ,  $c \triangleq \gamma_{\text{th}} \sqrt{P_s \hat{\gamma} (1 + \hat{\gamma})}$ ,  $d \triangleq P_s \hat{\gamma}$ ,  $\tilde{q} \triangleq \sqrt{P_s |h|^4 + d_1^m \sigma_r^2 |h|^2}$ ,  $u \triangleq d_1^m \sigma_r^2 \hat{\gamma}$ , and  $v \triangleq \sqrt{P_s \hat{\gamma} (1 + \hat{\gamma})}$ . Note that  $\hat{\gamma} < \gamma_{\text{SR}}$  indicates that the target relay can be implemented only when  $|h|^2 > \hat{\gamma} d_1^m \sigma_r^2 / P_s$ . Substituting  $f_{|f|^2}(z)$ ,  $f_{|h|^2}(z)$ ,

$F_{|g|^2}(z)$ , and  $|h|^2 > \hat{\gamma}d_1^m\sigma_r^2/P_s$  into (C.1), the outage probability can be written as

$$\begin{aligned} P_{\text{out}} &= \int_{w=0}^{\infty} \int_{z=0}^{\infty} f_{|f|^2}(w) f_{|h|^2}(z) \Pr \left( |g|^2 < -\frac{a\tilde{q}|f|^2}{(b|h|^2 - c\tilde{q})(d|h|^2 + u - \tilde{q}v)} \right) dz dw \\ &= 1 - \frac{1}{\lambda_f \lambda_h} \int_{w=0}^{\infty} \int_{z=\hat{\gamma}d_1^m\sigma_r^2/P_s}^{\infty} e^{-\frac{z}{\lambda_h} - \frac{w}{\lambda_f} + \frac{aqw}{(bz - cq)(dz + u - qv)\lambda_g}} dz dw, \end{aligned} \quad (\text{C.2})$$

where  $q = \sqrt{P_s z^2 + d_1^m \sigma_r^2 z}$ . The analytical expression in (C.2) cannot be further simplified. However,  $\sqrt{P_s |h|^4 + d_1^m \sigma_r^2 |h|^2} \approx \sqrt{P_s} |h|^2$  in high SINR. With the high SINR approximation,  $P_{\text{out}}$  can be approximated as

$$\begin{aligned} P_{\text{out}} &\approx \Pr \left( |g|^2 < \frac{a|f|^2 \sqrt{P_s}}{(c\sqrt{P_s} - b)((d - v\sqrt{P_s})|h|^2 + u)} \right) \\ &= \begin{cases} \Pr \left( |g|^2 < \frac{a|f|^2 \sqrt{P_s}}{(c\sqrt{P_s} - b)((d - v\sqrt{P_s})|h|^2 + u)} \right), & |h|^2 > \frac{u}{v\sqrt{P_s} - d}, \\ 1, & |h|^2 < \frac{u}{v\sqrt{P_s} - d}, \end{cases} \end{aligned} \quad (\text{C.3})$$

where the last equality follows similarly as that in (A.2) and  $|h|^2 > \frac{u}{v\sqrt{P_s} - d}$  also satisfies the condition of  $\hat{\gamma} < \gamma_{\text{SR}}$ . Then, using the similar procedure as that below (A.2), the outage probability approximation can be expressed as

$$\begin{aligned} P_{\text{out}} &\approx \int_{w=0}^{\infty} \int_{z=0}^{\frac{u}{v\sqrt{P_s} - d}} f_{|f|^2}(w) f_{|h|^2}(z) dz dw \\ &\quad + \int_{w=0}^{\infty} \int_{z=\frac{u}{v\sqrt{P_s} - d}}^{\infty} f_{|f|^2}(w) f_{|h|^2}(z) \Pr \left( |g|^2 < \frac{a|f|^2 \sqrt{P_s}}{(c\sqrt{P_s} - b)((d - v\sqrt{P_s})|h|^2 + u)} \right) dz dw \\ &= 1 - \frac{1}{\lambda_f \lambda_h} \int_{w=0}^{\infty} \int_{z=\frac{u}{v\sqrt{P_s} - d}}^{\infty} e^{-\frac{z}{\lambda_h} - \frac{w}{\lambda_f} - \frac{aw\sqrt{P_s}}{(c\sqrt{P_s} - b)((d - v\sqrt{P_s})z + u)\lambda_g}} dz dw \\ &\stackrel{(a)}{=} 1 - \frac{1}{\lambda_f} e^{-\frac{u}{(v\sqrt{P_s} - d)\lambda_h}} \int_0^{\infty} e^{-\frac{w}{\lambda_f}} \rho \sqrt{w} K_1(\rho \sqrt{w}) dw \\ &= 1 - e^{-\frac{u}{(v\sqrt{P_s} - d)\lambda_h}} (1 + \omega e^{\omega} (\text{Chi}(\omega) - \text{Shi}(\omega))), \end{aligned} \quad (\text{C.4})$$

where  $\rho = \sqrt{\frac{4a\sqrt{P_s}}{(b - c\sqrt{P_s})(v\sqrt{P_s} - d)\lambda_g \lambda_h}}$ ,  $\omega = \frac{a\sqrt{P_s} \lambda_f}{(b - c\sqrt{P_s})(v\sqrt{P_s} - d)\lambda_g \lambda_h}$ ,  $K_1(\cdot)$  is the first-order modified Bessel function of the second kind,  $\text{Shi}(\cdot)$  and  $\text{Chi}(\cdot)$  are the hyperbolic sine integral function and the hyperbolic cosine integral function, respectively [34, Eq. (8.2221)]. In (C.4), the step (a) follows similarly as that in (A.4)

## APPENDIX D

The ergodic capacity  $C_E = \mathbb{E}\{\log_2(1 + \gamma_{\max})\}$  can be expressed as

$$\begin{aligned} C_E &= \mathbb{E}\{\log_2(1 + \mu\gamma_{\text{RD}})\} + \mathbb{E}\{\log_2(1 + \gamma_{\text{SR}} + \mu\gamma_{\text{SR}}|f|^2)\} \\ &\quad - \mathbb{E}\{\log_2(1 + \gamma_{\text{SR}} + \mu\gamma_{\text{RD}} + \mu\gamma_{\text{SR}}|f|^2 + \mu^2\gamma_{\text{SR}}\gamma_{\text{RD}}|f|^2)\}. \end{aligned} \quad (\text{D.1})$$

Define  $x \triangleq |h|^2|g|^2$  and  $y \triangleq |h|^2(1 + \mu|f|^2)$ , the PDFs of  $x$  and  $y$  are given by  $f(x) = \frac{2}{\lambda_h\lambda_g}K_0\left(2\sqrt{\frac{x}{\lambda_h\lambda_g}}\right)$  and  $f(y) = \frac{2}{\lambda_h(1+\mu\lambda_f)}K_0\left(2\sqrt{\frac{y}{\lambda_h(1+\mu\lambda_f)}}\right)$ , respectively. Then, the first item could be evaluated as

$$\begin{aligned} \mathbb{E}\{\log_2(1 + \mu\gamma_{\text{RD}})\} &= \frac{2}{\lambda_h\lambda_g \ln 2} \int_0^\infty \ln\left(1 + \frac{\mu P_s x}{d_1^m d_2^m \sigma_d^2}\right) K_0\left(2\sqrt{\frac{x}{\lambda_h\lambda_g}}\right) dx \\ &\stackrel{(a)}{=} \frac{2}{\lambda_h\lambda_g \ln 2} \int_0^\infty G_{2,2}^{1,2}\left(\frac{\mu P_s x}{d_1^m d_2^m \sigma_d^2} \middle| \begin{smallmatrix} 1,1 \\ 1,0 \end{smallmatrix}\right) K_0\left(2\sqrt{\frac{x}{\lambda_h\lambda_g}}\right) dx \\ &\stackrel{(b)}{=} \frac{1}{\ln 2} G_{4,2}^{1,4}\left(\frac{\mu P_s \lambda_h \lambda_g}{d_1^m d_2^m \sigma_d^2} \middle| \begin{smallmatrix} 0,0,1,1 \\ 1,0 \end{smallmatrix}\right). \end{aligned} \quad (\text{D.2})$$

In (D.2), we have used the relationship [35, Eq. (8.4.6.5)] in the step (a) and the integral identity [34, Eq. (7.821.3)] in the step (b), respectively. Now, the second item can be shown similarly as

$$\mathbb{E}\{\log_2(1 + \gamma_{\text{SR}} + \mu\gamma_{\text{SR}}|f|^2)\} = \frac{1}{\ln 2} G_{4,2}^{1,4}\left(\frac{P_s \lambda_h (1+\mu\lambda_f)}{d_1^m \sigma_r^2} \middle| \begin{smallmatrix} 0,0,1,1 \\ 1,0 \end{smallmatrix}\right). \quad (\text{D.3})$$

The third item could be evaluated as

$$\begin{aligned} &\mathbb{E}\{\log_2(1 + \gamma_{\text{SR}} + \mu\gamma_{\text{RD}} + \mu\gamma_{\text{SR}}|f|^2 + \mu^2\gamma_{\text{SR}}\gamma_{\text{RD}}|f|^2)\} \\ &= \frac{1}{\lambda_h\lambda_g\lambda_f} \int_0^\infty \int_0^\infty \int_0^\infty e^{-\frac{z}{\lambda_h} - \frac{w}{\lambda_g} - \frac{v}{\lambda_f}} \xi(v, w, z) dz dw dv, \end{aligned} \quad (\text{D.4})$$

where  $\xi(v, w, z) \triangleq \log_2\left(1 + \frac{P_s z}{d_1^m \sigma_r^2} + \frac{\mu P_s z w}{d_1^m d_2^m \sigma_d^2} + \frac{\mu P_s z v}{d_1^m \sigma_r^2} + \frac{\mu^2 P_s^2 z^2 w v}{d_1^{2m} d_2^m \sigma_r^2 \sigma_d^2}\right)$ . Then, the desired result follows immediately.

## APPENDIX E

This part derives the ergodic capacity achieved by the optimal relay gain. According to (B.2), the CDF of  $\gamma_{\text{opt}}$ ,  $F_{\gamma_{\text{opt}}}(\gamma)$ , is given by

$$F_{\gamma_{\text{opt}}}(\gamma) = 1 - \frac{1}{\lambda_f \lambda_h} \int_0^\infty \left( \frac{az+b+c\sqrt{z(P_s z+d)}}{(P_s z-\gamma d)^2 \lambda_g} + \frac{1}{\lambda_f} \right)^{-1} e^{-\frac{z}{\lambda_h}} dz, \quad (\text{E.1})$$

where  $a \triangleq P_s d_1^m d_2^m \sigma_d^2 \gamma (1 + 2\gamma)$ ,  $b \triangleq d_1^{2m} d_2^m \sigma_r^2 \sigma_d^2 \gamma^2$ , and  $c \triangleq 2d_1^m d_2^m \sigma_d^2 \gamma \sqrt{P_s \gamma (1 + \gamma)}$ , and  $d \triangleq d_1^m \sigma_r^2$ . Then, the PDF of  $\gamma_{\text{opt}}$  can be computed by

$$\begin{aligned} f_{\gamma_{\text{opt}}}(\gamma) &= \frac{\partial F_{\gamma_{\text{opt}}}(\gamma)}{\partial \gamma} \\ &= -\frac{1}{\lambda_f \lambda_h} \int_0^\infty \frac{\partial}{\partial \gamma} \left[ \left( \frac{az + b + c\sqrt{z(P_s z + d)}}{(P_s z - \gamma d)^2 \lambda_g} + \frac{1}{\lambda_f} \right)^{-1} \right] e^{-\frac{z}{\lambda_h}} dz. \end{aligned} \quad (\text{E.2})$$

Using (E.2), the ergodic capacity  $C_E = \mathbb{E}\{\log_2(1 + \gamma)\}$  can be expressed as

$$\begin{aligned} C_E &= \int_{\gamma=0}^\infty f_{\gamma_{\text{opt}}}(\gamma) \log_2(1 + \gamma) d\gamma \\ &= -\frac{1}{\lambda_f \lambda_h} \int_0^\infty \int_0^\infty \frac{\partial}{\partial \gamma} \left[ \left( \frac{az + b + c\sqrt{z(P_s z + d)}}{(P_s z - \gamma d)^2 \lambda_g} + \frac{1}{\lambda_f} \right)^{-1} \right] e^{-\frac{z}{\lambda_h}} \log_2(1 + \gamma) dz d\gamma. \end{aligned} \quad (\text{E.3})$$

The analytical result presented in (E.3) has a very large expression and its close-form can hardly be obtained. However, high SINR approximation can be applied to (E.3), as earlier explained below (B.2) in Appendix B. Therefore, following (B.3) and (B.4), the approximation of (E.1) can be expressed as

$$F_{\gamma_{\text{opt}}}(\gamma) \approx 1 - e^{-\frac{v}{\lambda_h}} - e^\rho \left( \rho + \frac{v}{\lambda_h} \right) E_i \left( -\rho - \frac{v}{\lambda_h} \right), \quad (\text{E.4})$$

where  $v = \frac{2d_1^m \sigma_r^2 \gamma}{P_s}$  and  $\rho = \frac{\lambda_f(a + c\sqrt{P_s}) - 2\lambda_g P_s d_1^m \sigma_r^2 \gamma}{\lambda_g \lambda_h P_s^2}$ . By evaluating the derivative of  $F_{\gamma_{\text{opt}}}(\gamma)$  in (E.4) with respect to  $\gamma$ , the approximate value for the PDF of  $\gamma_{\text{opt}}$  can be written as

$$f_{\gamma_{\text{opt}}}(\gamma) = \frac{v}{\gamma \lambda_h} e^{-\frac{v}{\lambda_h}} - \tilde{a} e^{\rho - \omega} - \left( \tilde{b} \left( \rho + \frac{v}{\lambda_h} \right) e^{\frac{\rho}{P_s^2}} + \tilde{c} e^{\rho + \omega} \right) E_i \left( -\rho - \frac{v}{\lambda_h} \right), \quad (\text{E.5})$$

where  $\tilde{a} \triangleq \frac{(1 + \gamma + \sqrt{\gamma(1 + \gamma)})(\lambda_h \rho + v)}{\lambda_h \gamma (1 + \gamma)}$ ,  $\tilde{b} \triangleq -\frac{2d}{P_s \lambda_h} + \frac{\lambda_f}{P_s \lambda_h \lambda_g} \left( \frac{b(3 + 4\gamma)}{\gamma \sqrt{\gamma(1 + \gamma)} \sigma_r^2} + d_1^m d_2^m (1 + 4\gamma) \sigma_d^2 \right)$ ,  $\tilde{c} \triangleq \frac{\lambda_f (2b\sqrt{P_s}(3 + 4\gamma) + c(1 + 4\gamma)\sigma_r^2)}{2P_s \lambda_h \lambda_g \gamma \sqrt{P_s \gamma(1 + \gamma)} \sigma_r^2}$ , and  $\omega \triangleq \frac{(a + c\sqrt{P_s})\lambda_f}{P_s^4 \lambda_h \lambda_g}$ . Then, the approximation of the ergodic capacity achieved with  $\beta_{\text{opt}}$  can be expressed as

$$C_E \approx \int_0^\infty \left( \frac{v}{\gamma \lambda_h} e^{-\frac{v}{\lambda_h}} - \tilde{a} e^{\rho - \omega} - \left( \tilde{b} \left( \rho + \frac{v}{\lambda_h} \right) e^{\frac{\rho}{P_s^2}} + \tilde{c} e^{\rho + \omega} \right) E_i \left( -\rho - \frac{v}{\lambda_h} \right) \right) \log_2(1 + \gamma) d\gamma. \quad (\text{E.6})$$

## APPENDIX F

This part derives Proposition 6. The ergodic capacity achieved by the target relay gain can be written as

$$\begin{aligned} C_E &= \mathbb{E}\{\log_2(1 + \gamma_{\text{tar}})\} \\ &= \mathbb{E}\{\log_2(1 + \gamma_{\text{tar},1})\} - \mathbb{E}\{\log_2(1 + \gamma_{\text{tar},2})\}, \end{aligned} \quad (\text{F.1})$$

where  $\gamma_{\text{tar},1} \triangleq \frac{P_s x}{d_1^m d_2^m \hat{\gamma} \sigma_r^2 \sigma_d^2} + \frac{P_s^2(1+\hat{\gamma}-\sqrt{\hat{\gamma}(1+\hat{\gamma})})y}{d_1^{2m} d_2^m \hat{\gamma} \sigma_r^2 \sigma_d^2}$ ,  $\gamma_{\text{tar},2} \triangleq \frac{P_s x}{d_1^m d_2^m \hat{\gamma} \sigma_r^2 \sigma_d^2} + \frac{P_s^2(1+2\hat{\gamma}-2\sqrt{\hat{\gamma}(1+\hat{\gamma})})y}{d_1^{2m} d_2^m \hat{\gamma} \sigma_r^2 \sigma_d^2}$ ,  $x \triangleq \frac{|h|^2(a|g|^2+b|f|^2)}{|f|^2}$ ,  $y \triangleq \frac{|g|^2|h|^4}{|f|^2}$ ,  $a \triangleq (\sqrt{\hat{\gamma}(1+\hat{\gamma})}-\hat{\gamma})\sigma_r^2$ , and  $b \triangleq d_2^m \sigma_d^2 \sqrt{\hat{\gamma}(1+\hat{\gamma})}$ . Based on the fact that  $f(x, y) = \log_2(1 + e^x + e^y)$  is a convex function with respect to  $x$  and  $y$ , we have

$$\mathbb{E}\{\log_2(1 + \gamma_{\text{tar},1})\} \geq \log_2 \left( 1 + \frac{P_s}{d_1^m d_2^m \hat{\gamma} \sigma_r^2 \sigma_d^2} e^{\mathbb{E}\{\ln x\}} + \frac{P_s^2(1+\hat{\gamma}-\sqrt{\hat{\gamma}(1+\hat{\gamma})})}{d_1^{2m} d_2^m \hat{\gamma} \sigma_r^2 \sigma_d^2} e^{\mathbb{E}\{\ln y\}} \right) \quad (\text{F.2})$$

and

$$\mathbb{E}\{\log_2(1 + \gamma_{\text{tar},2})\} \geq \log_2 \left( 1 + \frac{P_s}{d_1^m d_2^m \hat{\gamma} \sigma_r^2 \sigma_d^2} e^{\mathbb{E}\{\ln x\}} + \frac{P_s^2(1+2\hat{\gamma}-2\sqrt{\hat{\gamma}(1+\hat{\gamma})})}{d_1^{2m} d_2^m \hat{\gamma} \sigma_r^2 \sigma_d^2} e^{\mathbb{E}\{\ln y\}} \right), \quad (\text{F.3})$$

respectively. Subject to the constraint of  $\hat{\gamma} < \gamma_{\text{SR}}$ , i.e.,  $|h|^2 > \hat{\gamma} d_1^m \sigma_r^2 / P_s$ , the item  $\mathbb{E}\{\ln x\}$  can be evaluated as

$$\begin{aligned} \mathbb{E}\{\ln x\} &= \frac{1}{\lambda_h \lambda_g \lambda_f} \int_{t=0}^{\infty} \int_{w=0}^{\infty} \int_{z=\hat{\gamma} d_1^m \sigma_r^2 / P_s}^{\infty} e^{-\frac{z}{\lambda_h} - \frac{w}{\lambda_g} - \frac{t}{\lambda_f}} \ln \left( \frac{z(aw+bt)}{t} \right) dz dw dt \\ &= -E_i \left( -\frac{\hat{\gamma} d_1^m \sigma_r^2}{\lambda_h P_s} \right) + \frac{1}{\lambda_g \lambda_f} e^{-\frac{\hat{\gamma} d_1^m \sigma_r^2}{\lambda_h P_s}} \int_{t=0}^{\infty} \int_{w=0}^{\infty} e^{-\frac{w}{\lambda_g} - \frac{t}{\lambda_f}} \ln \left( \frac{d_1^m \hat{\gamma} \sigma_r^2 (aw+bt)}{P_s t} \right) dw dt \\ &\stackrel{(a)}{=} -E_i \left( -\frac{\hat{\gamma} d_1^m \sigma_r^2}{\lambda_h P_s} \right) + \frac{1}{\lambda_f} e^{-\frac{\hat{\gamma} d_1^m \sigma_r^2}{\lambda_h P_s}} \int_{t=0}^{\infty} e^{-\frac{t}{\lambda_f}} \left( -e^{\frac{bt}{a\lambda_g}} E_i \left( -\frac{bt}{a\lambda_g} \right) + \ln \left( \frac{b\hat{\gamma} d_1^m \sigma_r^2}{P_s} \right) \right) dt \\ &\stackrel{(b)}{=} -E_i \left( -\frac{\hat{\gamma} d_1^m \sigma_r^2}{\lambda_h P_s} \right) + e^{-\frac{\hat{\gamma} d_1^m \sigma_r^2}{\lambda_h P_s}} \left( \frac{1}{a\lambda_g - b\lambda_f} a\lambda_g \ln \left( \frac{a\lambda_g}{b\lambda_f} \right) + \ln \left( \frac{b\hat{\gamma} d_1^m \sigma_r^2}{P_s} \right) \right). \end{aligned} \quad (\text{F.4})$$

In (F.4), the relationship [35, Eq. (8.4.6.5)] has been used in the step (a) and the relationship [34, Eq. (6.224)] has been used in the step (b). Similarly, the item  $\mathbb{E}\{\ln y\}$  can be computed as

$$\begin{aligned} \mathbb{E}\{\ln y\} &= \frac{1}{\lambda_h \lambda_g \lambda_f} \int_{t=0}^{\infty} \int_{w=0}^{\infty} \int_{z=\hat{\gamma} d_1^m \sigma_r^2 / P_s}^{\infty} e^{-\frac{z}{\lambda_h} - \frac{w}{\lambda_g} - \frac{t}{\lambda_f}} \ln \left( \frac{wz^2}{t} \right) dz dw dt \\ &= \frac{1}{\lambda_g \lambda_f} \int_{t=0}^{\infty} \int_{w=0}^{\infty} e^{-\frac{t}{\lambda_f} - \frac{w}{\lambda_g} - \frac{\hat{\gamma} d_1^m \sigma_r^2}{\lambda_h P_s}} \left( \ln \left( \frac{w\hat{\gamma}^2 d_1^{2m} \sigma_r^4}{P_s^2 t} \right) - 2e^{\frac{\hat{\gamma} d_1^m \sigma_r^2}{\lambda_h P_s}} E_i \left( -\frac{\hat{\gamma} d_1^m \sigma_r^2}{\lambda_h P_s} \right) \right) dw dt \\ &= \frac{1}{\lambda_f} \int_{t=0}^{\infty} e^{-\frac{t}{\lambda_f} - \frac{\hat{\gamma} d_1^m \sigma_r^2}{\lambda_h P_s}} \left( \ln \left( \frac{\lambda_g \hat{\gamma}^2 d_1^{2m} \sigma_r^4}{P_s^2 t} \right) + \psi(1) - 2e^{\frac{\hat{\gamma} d_1^m \sigma_r^2}{\lambda_h P_s}} E_i \left( -\frac{\hat{\gamma} d_1^m \sigma_r^2}{\lambda_h P_s} \right) \right) dt \\ &= -2E_i \left( -\frac{\hat{\gamma} d_1^m \sigma_r^2}{\lambda_h P_s} \right) - e^{-\frac{\hat{\gamma} d_1^m \sigma_r^2}{\lambda_h P_s}} \ln \left( \frac{\lambda_f P_s^2}{\lambda_g \hat{\gamma}^2 d_1^{2m} \sigma_r^4} \right). \end{aligned} \quad (\text{F.5})$$

This proves Proposition 6.

## REFERENCES

- [1] W. K. G. Seah, Z. A. Eu, and H. P. Tan, "Wireless sensor networks powered by ambient energy harvesting (WSN-HEAP) - survey and challenges," in *Proc. Wireless VITAE 2009*, Aalborg, Denmark, May 2009, pp. 1–5.

- [2] C. Huang, R. Zhang, and S. Cui, "Throughput maximization for the gaussian relay channel with energy harvesting constraints," *IEEE J. Sel. Areas in Commun.*, vol. 31, no. 8, pp. 1469–1479, Aug. 2013.
- [3] D. T. Hoang, D. Niyato, P. Wang, and D. I. Kim, "Opportunistic channel access and RF energy harvesting in cognitive radio networks," *IEEE J. Sel. Areas in Commun.*, vol. 32, no. 11, pp. 2039–2052, Nov. 2014.
- [4] J. Xu and R. Zhang, "Throughput optimal policies for energy harvesting wireless transmitters with non-ideal circuit power," *IEEE J. Sel. Areas in Commun.*, vol. 32, no. 2, pp. 322–332, Feb. 2014.
- [5] L. R. Varshney, "Transporting information and energy simultaneously," in *Proc. IEEE ISIT 2008*, Toronto, Canada, July 2008, pp. 1612–1616.
- [6] P. Grover and A. Sahai, "Shannon meets tesla: Wireless information and power transfer," in *Proc. IEEE ISIT 2010*, Austin, Tx, June 2010, pp. 2363–2367.
- [7] X. Zhou, R. Zhang, and C. K. Ho, "Wireless information and power transfer: Architecture design and rate-energy tradeoff," *IEEE Trans. Commun.*, vol. 61, no. 11, pp. 4754–4767, Nov. 2013.
- [8] K. Huang and V. Lau, "Enabling wireless power transfer in cellular networks: Architecture, modeling and deployment," *IEEE Trans. Wireless Commun.*, vol. 13, no. 2, pp. 902–912, Feb. 2014.
- [9] I. Krikidis, S. Timotheou, S. Nikolaou, G. Zheng, D. Ng, and R. Schober, "Simultaneous wireless information and power transfer in modern communication systems," *IEEE Commun. Mag.*, vol. 52, no. 11, pp. 104–110, Nov. 2014.
- [10] A. Nasir, X. Zhou, S. Durrani, and R. Kennedy, "Throughput and ergodic capacity of wireless energy harvesting based df relaying network," in *Proc. IEEE ICC 2014*, Sydney, Australia, June 2014, pp. 4066–4071.
- [11] —, "Relaying protocols for wireless energy harvesting and information processing," *IEEE Trans. Wireless Commun.*, vol. 12, no. 7, pp. 3622–3636, Jul. 2013.
- [12] Z. Xiang and M. Tao, "Robust beamforming for wireless information and power transmission," *IEEE Wireless Commun. Lett.*, vol. 1, no. 4, pp. 372–375, Aug. 2012.
- [13] A. Fouladgar and O. Simeone, "On the transfer of information and energy in multi-user systems," *IEEE Commun. Lett.*, vol. 16, no. 11, pp. 1733–1736, Nov. 2012.
- [14] P. Popovski, A. Fouladgar, and O. Simeone, "Interactive joint transfer of energy and information," *IEEE Trans. Commun.*, vol. 61, no. 5, pp. 2086–2097, May 2013.
- [15] R. Zhang and C. K. Ho, "Mimo broadcasting for simultaneous wireless information and power transfer," *IEEE Trans. Wireless Commun.*, vol. 12, no. 5, pp. 1989–2001, May 2013.
- [16] D. W. K. Ng, E. S. Lo, and R. Schober, "Energy-efficient resource allocation in multiuser ofdm systems with wireless information and power transfer," in *Proc. IEEE WCNC 2013*, Shanghai, China, April 2013, pp. 3823–3828.
- [17] G. Du, K. Xiong, Y. Zhang, and Z. Qiu, "Outage analysis and optimization for time switching-based two-way relaying with energy harvesting relay node," *KSII Transactions on Internet and Information System*, vol. 9, no. 2, pp. 545–563, 2014.
- [18] G. Du, Z. Dong, K. Xiong, and Z. Qiu, "Wireless information and energy transfer for decode-and-forward relying MIMO-OFDM networks," *to appear in ICIC Express Letters*.
- [19] K. Xiong, P. Fan, C. Zhang, and K. B. Letaief, "Wireless information and energy transfer for two-hop non-regenerative MIMO-OFDM relay networks," *IEEE J. Sel. Areas in Commun.*, pp. 1–17, Jan. 2015.
- [20] A. A. Nasir, X. Zhou, S. Durrani, and R. A. Kennedy, "Wireless energy harvesting and information relaying: Adaptive time-switching protocols and throughput analysis," 2013. [Online]. Available: <http://arxiv.org/abs/1310.7648>.

- [21] Z. Ding, S. Perlaza, I. Esnaola, and H. Poor, "Power allocation strategies in energy harvesting wireless cooperative networks," *IEEE Trans. Wireless Commun.*, vol. 13, no. 2, pp. 846–860, Feb. 2014.
- [22] Z. Ding, I. Krikidis, B. Sharif, and H. Poor, "Wireless information and power transfer in cooperative networks with spatially random relays," *IEEE Trans. Wireless Commun.*, vol. 13, no. 8, pp. 4440–4453, Aug. 2014.
- [23] H. Chen, Y. Li, Y. Jiang, Y. Ma, and B. Vucetic, "Distributed power splitting for swipt in relay interference channels using game theory," *IEEE Trans. Wireless Commun.*, vol. 14, no. 1, pp. 410–420, Aug. 2014.
- [24] I. Krikidis, S. Sasaki, S. Timotheou, and Z. Ding, "A low complexity antenna switching for joint wireless information and energy transfer in mimo relay channels," *IEEE Trans. Commun.*, vol. 62, no. 5, pp. 1577–1587, May 2014.
- [25] Z. Zhou, M. Peng, Z. Zhao, and Y. Li, "Joint power splitting and antenna selection in energy harvesting relay channels," *IEEE Trans. Signal Process.*, vol. 22, no. 7, pp. 823–827, Jul. 2015.
- [26] A. Sabharwal, P. Schniter, D. Guo, D. Bliss, S. Rangarajan, and R. Wichman, "In-band full-duplex wireless: Challenges and opportunities," *IEEE J. Sel. Areas in Commun.*, vol. 32, no. 9, pp. 1637–1652, Sept. 2014.
- [27] T. Riihonen, S. Werner, and R. Wichman, "Hybrid full-duplex/half-duplex relaying with transmit power adaptation," *IEEE Trans. Wireless Commun.*, vol. 10, no. 9, pp. 3074–3085, Sep. 2011.
- [28] C. Zhong, H. Suraweera, G. Zheng, I. Krikidis, and Z. Zhang, "Wireless information and power transfer with full duplex relaying," *IEEE Trans. Commun.*, vol. 62, no. 10, pp. 3447–3461, Oct. 2014.
- [29] G. Liu, H. Ji, F. Yu, Y. Li, and R. Xie, "Energy-efficient resource allocation in full-duplex relaying networks," in *Proc. IEEE ICC 2014*, Sydney, Australia, Jun. 2014, pp. 2400–2405.
- [30] H. Kim, S. Lim, H. Wang, and D. Hong, "Optimal power allocation and outage analysis for cognitive full duplex relay systems," *IEEE Trans. Wireless Commun.*, vol. 11, no. 10, pp. 3754–3765, Oct. 2012.
- [31] Femto Forum, "Interference Management in UMTS Femtocells," February 2010.
- [32] Y. Zeng and R. Zhang, "Full-duplex wireless-powered relay with self-energy recycling," *IEEE Wireless Commun. Lett.*, vol. PP, no. 99, pp. 1–1, 2015.
- [33] T. Riihonen, S. Werner, and R. Wichman, "Optimized gain control for single-frequency relaying with loop interference," *IEEE Trans. Wireless Commun.*, vol. 8, no. 6, pp. 2801–2806, Jun. 2009.
- [34] I. S. Gradshteyn and I. M. Ryzhik, *Table of Integrals, Series, and Products*. New York: Academic Press, 2007.
- [35] A. P. Prudnikov, Y. A. Brychkov, and O. I. Marichev, *Integrals and Series, Volumn 3: More Special Functions*. New York: Gordon and Breach Science, 1990.



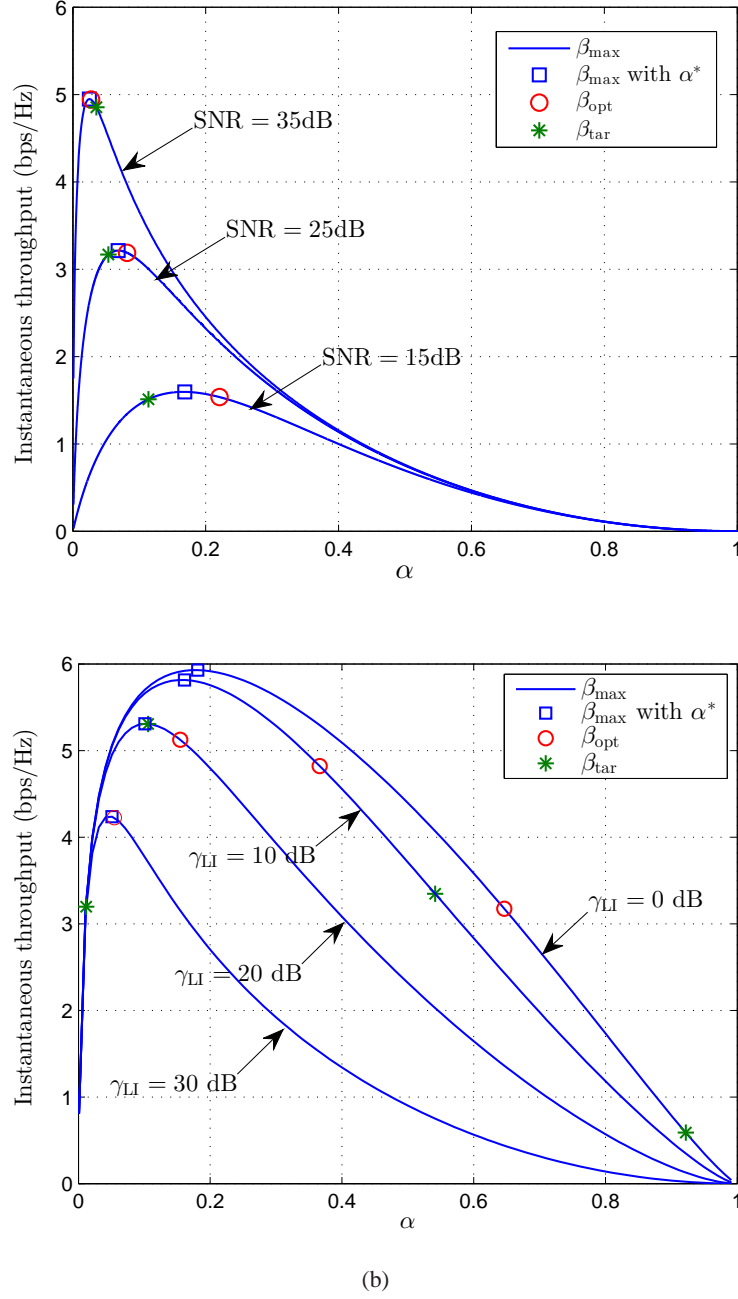
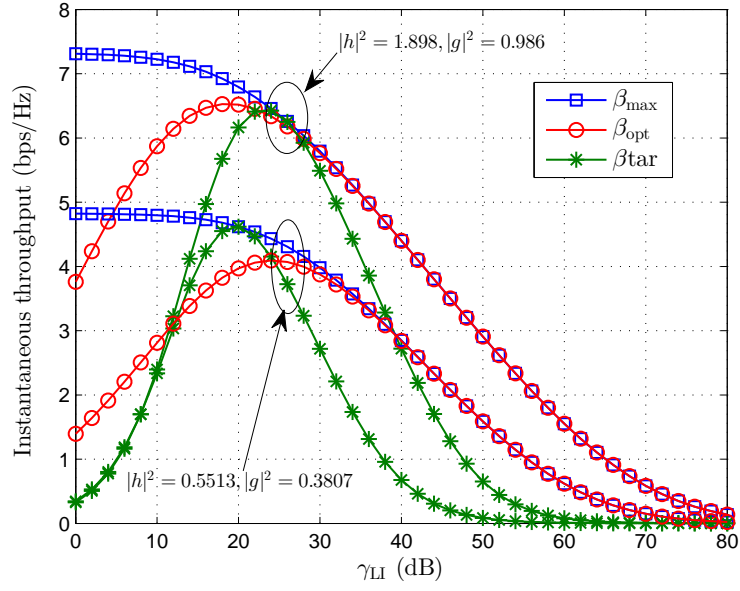
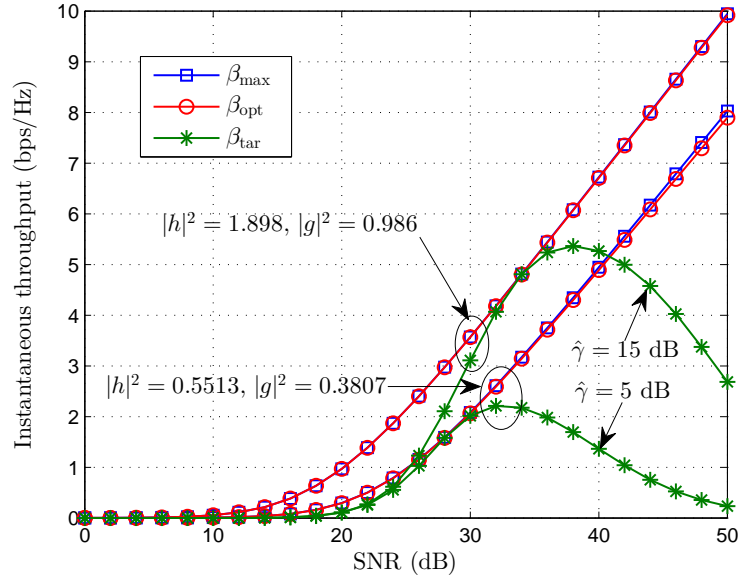


Fig. 2. Instantaneous capacity versus  $\alpha$ .



(a) Instantaneous throughput versus  $\gamma_{LI}$ :  $\hat{\gamma} = 25$  dB and  $\hat{\gamma} = 22$  dB



(b) Instantaneous throughput versus SNR:  $\gamma_{LI} = 35$  dB

Fig. 3. The instantaneous throughput performance.

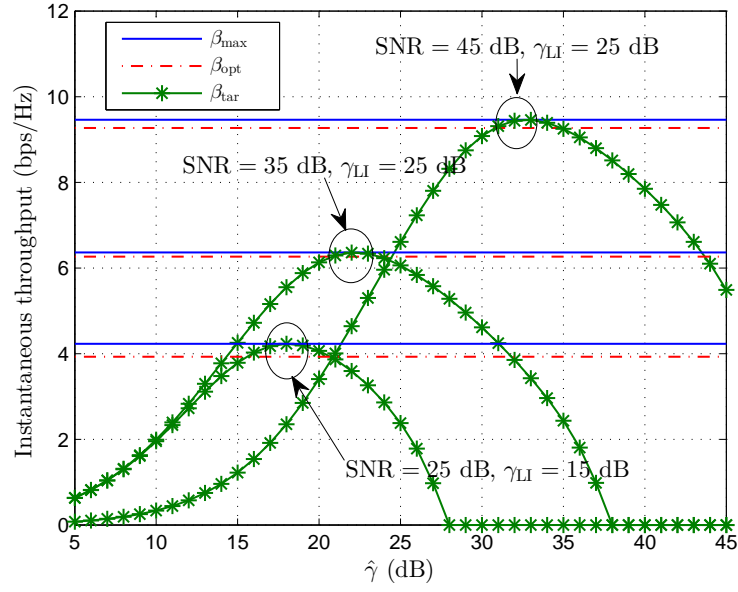


Fig. 4. Instantaneous throughput versus  $\hat{\gamma}$ .

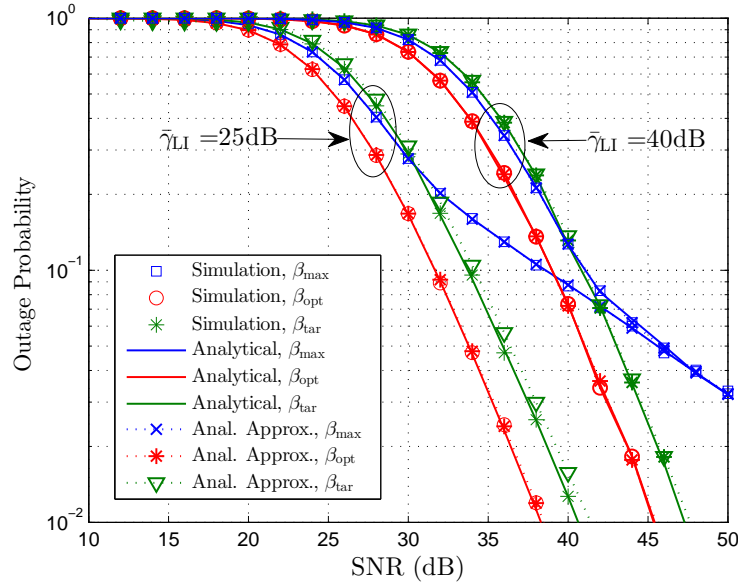


Fig. 5. Outage probability versus SNR.

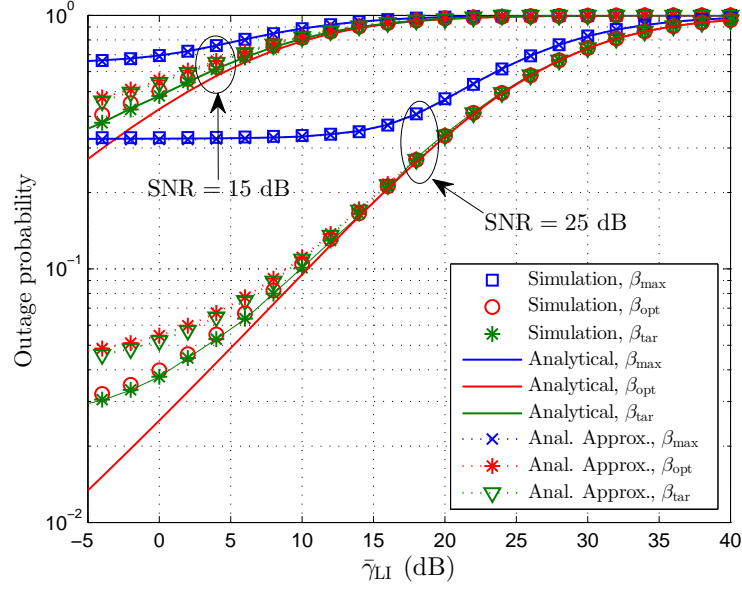


Fig. 6. Outage probability versus  $\bar{\gamma}_{LI}$ .

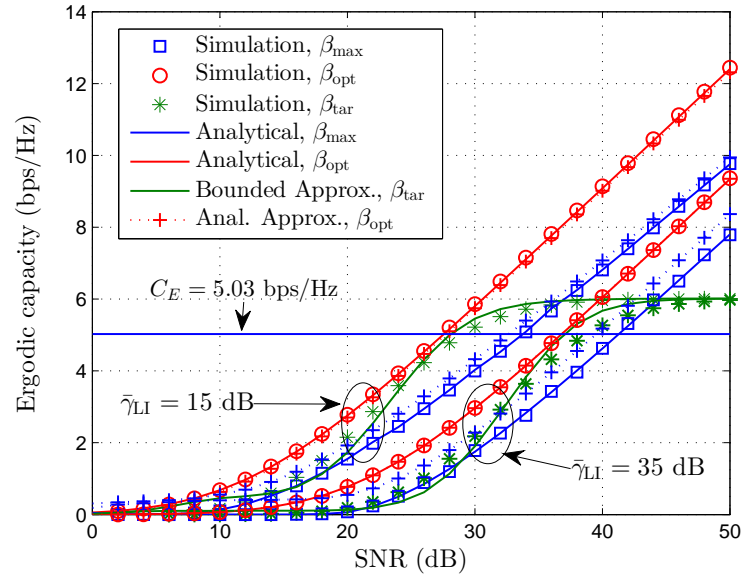


Fig. 7. Ergodic capacity versus SNR.

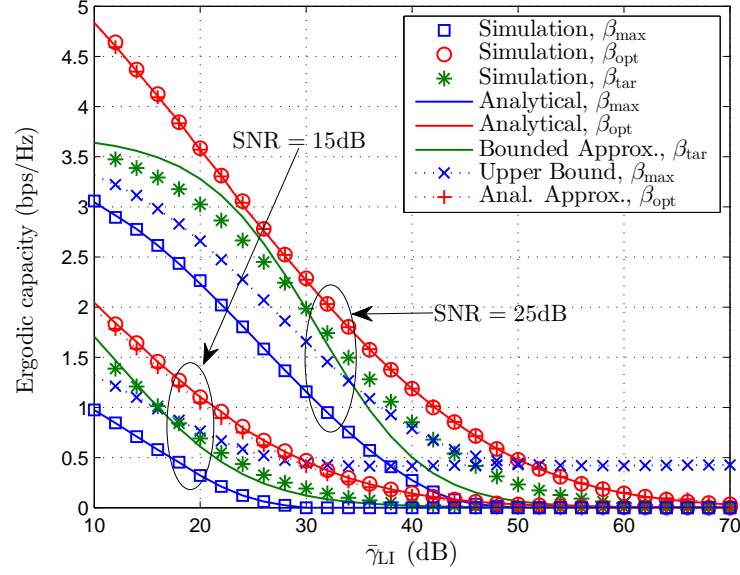


Fig. 8. Ergodic capacity versus  $\bar{\gamma}_{LI}$ .

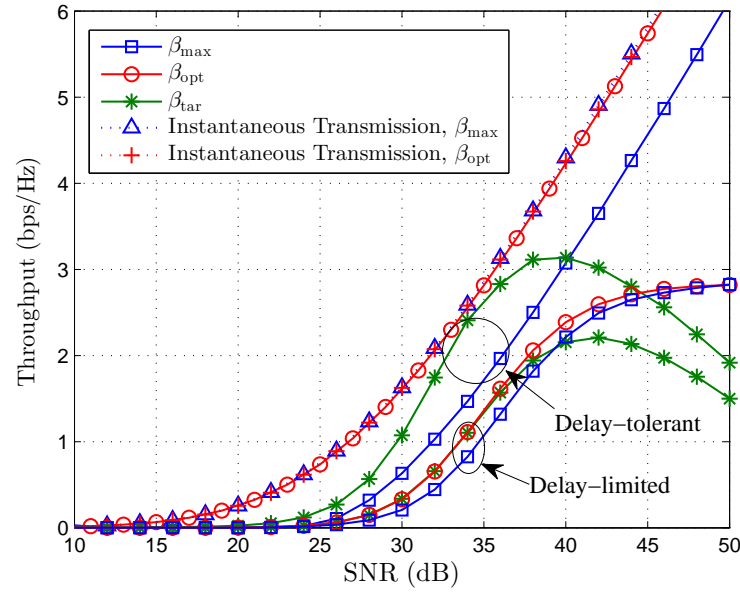


Fig. 9. Throughput versus SNR.

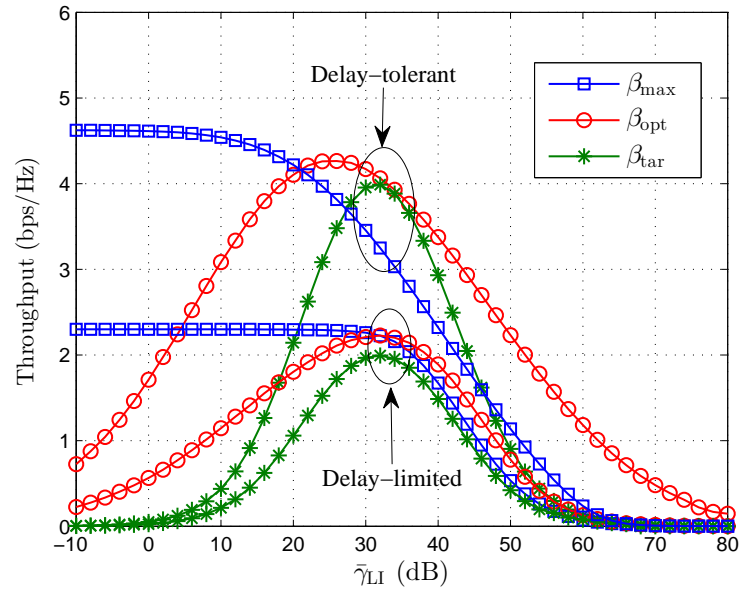
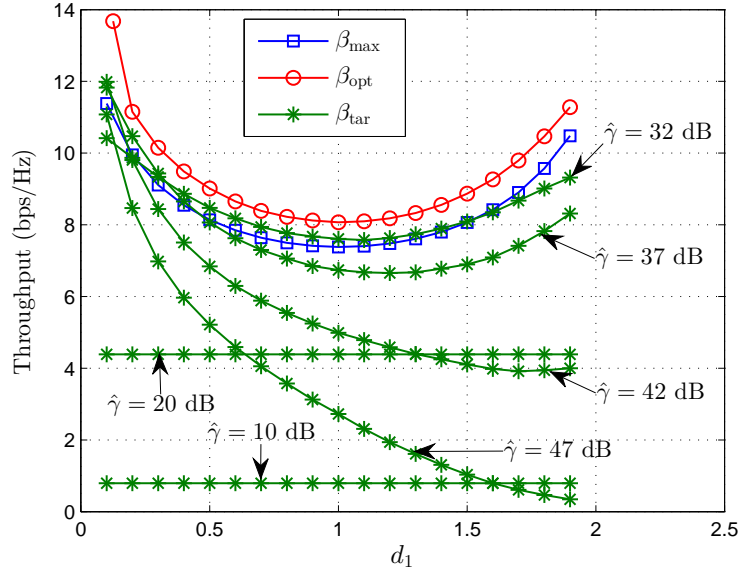
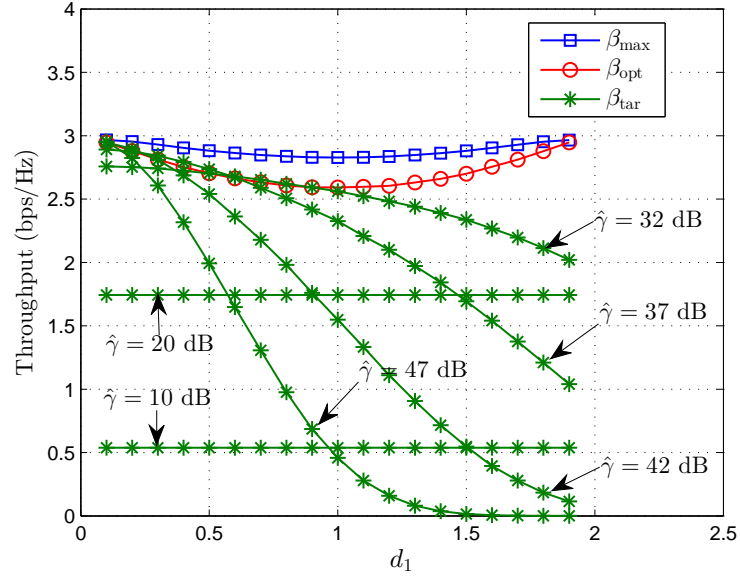


Fig. 10. Throughput versus  $\bar{\gamma}_{LI}$ .



(a) Delay tolerant mode



(b) Delay-limited mode.

Fig. 11. Throughput versus  $d_1$ .